ABSTRACT

Title of Document: TEMPERATURE AND PRESSURE EFFECTS ON HYDROGEN PERMEATION IN PALLADIUM BASED MEMBRANES.

Ryan T. James, Master of Science, 2010

Directed By: Professor Ashwani K. Gupta
Department of Mechanical Engineering

Palladium based membranes offer a promising method for extracting hydrogen from multi-component synthetic gas (syngas) mixtures. Thin palladium and palladium alloy membranes supported on porous media combine both enhanced strength and durability with increased permeation. The syngas produced from waste and biomass contains several gases of different concentrations. The availability of clean hydrogen from syngas is novel since the hydrogen storage and transportation are amongst the major issues for the utilization of hydrogen. A lab scale experimental facility has been designed and built that allows one to examine different types of membranes for efficient and effective separation of hydrogen from syngas. Experimental results have been obtained from this facility using palladium membranes. The results show hydrogen permeation increased with both temperature and pressure, with the greatest increase occurring with rising temperature. Determination of the pressure exponent revealed that the reaction was limited by both the surface reaction and diffusion process.

TEMPERATURE AND PRESSURE EFFECTS ON HYDROGEN PERMEATION IN PALLADIUM BASED MEMBRANES.

By

Ryan T. James

Thesis submitted to the Faculty of the Graduate School of the
University of Maryland, College Park, in partial fulfillment
of the requirements for the degree of
Master of Science
2010

Advisory Committee:
Professor Ashwani K. Gupta, Chair
Dr. Bao Yang, Associate Professor
Dr. Nam Sun Wang, Associate Professor

Acknowledgements

I would like to take this opportunity to thank my advisor, Dr. Ashwani Gupta, for providing me with the opportunity to come to the University of Maryland as his advisee for the past two years. He provided me with a great opportunity to do research in a field of escalating interest and importance for future energy needs. Dr. Gupta gave me his full support and offered guidance from his own experiences gained over his long and successful career. I am very appreciative for all that he has done to provide me with the necessary tools to have achieved so much success in my short two year time span at the University of Maryland. I'd like to thank Dr. Shamsuddin Ilias and his research team at North Carolina A&T State University for their assistance in providing the membranes for this study. I would also like to thank my advisory committee, Dr. Bao Yang and Dr. Nam Sun Wang, for so graciously being a part of my committee.

I could never have survived these past two years without the assistance of the members of the Combustion Laboratory at the University of Maryland: Ahmed Abdelhafez, Ahmed Khalil, Hatem Selim, Henry Molintas, Islam Ahmed, Vaibhav Arghode, Vineeth Vijayan, and Vivek Shirsat. Not only did they help me along the way in terms of academics and research, but they have also been true friends. I especially thank Islam for his guidance in helping me learn how to design and run experiments. I came to the University of Maryland with very little research experience, but Islam sacrificed hours of his personal time to ensure I was moving in the right direction.

I would also like to thank the United States Coast Guard for accepting me to the Naval Engineering Postgraduate (NEPG) Program. Particularly, I'd like to show my appreciation for the guidance and support provided by CAPT Mike Mohn, CAPT Caleb Corson, CDR James Passarelli, LCDR Mike Adams and LT Kenneth Boyt. They've been exceptional mentors and are without a doubt a major reason for the early success in my Coast Guard career that led to my acceptance by the NEPG.

I would like to thank my parents, George and Michelle James, for their loving support and confidence. They've always been a huge motivation and have always believed I could achieve anything. I thank my brother Todd for his advice and support along the way, and my brother Greg, who even after his passing over five years ago, still serves as a daily inspiration in my life. I would like to acknowledge the rest of my family and friends who have been there for me over the years and supported me through my time at Maryland. Lastly, but surely not least, I would like to thank my beautiful wife, Megan. Her unwavering support accompanied by her persistent patience these past two years have been a blessing. I'm truly grateful for the sacrifices she's made so I could have this opportunity.

Table of Contents

List of Tables

List of Figures

Chapter 1: Motivation and Objectives

The complications surrounding the separation of hydrogen gas from multi-component gas mixtures have long presented challenges for engineers. While the concept of hydrogen separation has been around for several decades, it is not a very widely used process. Improvements in this technique are sought in an effort to increase the amount of hydrogen available as a fuel source for current as well as future applications.

Every since its discovery as a barrier permeable only by hydrogen in the 1860's, palladium has been the most commonly used material for hydrogen separation. For the past 150 years, palladium has been tested at various temperatures, pressures, and compositions. Researchers have tried several palladium alloys in an effort to find a cheap yet dependable separation barrier. Cost most often times ends up being one of the largest limiting factors in industrial scale hydrogen separation. Often times the cost of the materials and facilities are not recouped by resulting hydrogen production. Dependability has been another problem associated with hydrogen separation as the short lifespan of membranes also increases cost.

The high cost is the main problem facing engineers working with hydrogen separation, but it is only the tip of the iceberg. If a lot of the underlying issues are resolved, the cost problem will be drastically diminished. This is why the search for cheaper membrane materials without sacrificing productivity, or if possible, improving productivity, has been such major goal for researchers. Membrane durability is another key issue. How well will the membrane stand up to high

pressures? Or high temperatures? What about multi-gas mixtures? How do you make the membrane stronger without a sacrificing hydrogen production?

Recognizing the need is first step in attempting to solve any problem. In the case of hydrogen separation, the need is a better understanding of the hydrogen diffusion process across various material compositions under changing environmental conditions, as the above questions indicate. While this need is very general, it applies to the hydrogen separation principle as a whole. For this project, the need was focused more precisely on the effects of testing palladium based membranes at various temperatures and pressures. The problem, therefore, was recognizing the effects and determining their relevance to the overall hydrogen permeation process.

The first objective of this study was to develop an experimental facility with which membranes could be tested. The research and design process for the facility used in this project are contained within this study. The next objective was to test the facility under the desired operational conditions. All tests were documented and any problems were identified or corrected. The third objective was to test for membrane integrity. That is, make sure that nothing goes through the membrane except hydrogen. Contained within this thesis are detailed results of the integrity testing and causes for any detected leakage. The final objective was to identify the effects of varying temperature and pressure on the hydrogen permeation through the palladium based membranes. A comprehensive account of the experimental results is contained within this study, including the parameter variation effects on leaks in the membrane surface and hydrogen permeation, determination of the pressure exponent, and calculation of the activation energy and permeability constant. Also included in this

study are all assumptions made and the reasoning behind each assumption. A thorough uncertainty analysis was also conducted and applied to the experimental data.

Chapter 2: Literature Review

There are three primary categories associated with hydrogen separation techniques: physical, chemical, and selective diffusion. Chemical separation uses a catalytic purification technique and physical separation involves metal hydride separation, pressure swing adsorption, and cryogenic separation [1]. Selective diffusion uses various types of membranes, namely noble metal and polymer based membranes [1]. The operating conditions as well as output preferences are key factors in determining the preferred method.

Since the center piece of this thesis is palladium based membranes, this chapter will focus on palladium membrane diffusion. There will be a rather thorough description of the diffusion method and the chemical kinetics involved, including an overview of both Sievert's and Fick's laws. Operating parameters will be addressed based on previous experimental studies. These results will be further examined based on whether the goal was to have the optimum hydrogen quantity, purity, or a balance of both. The material composition of the membrane will also be examined, including a direct correlation between the membrane composition, the operating parameters and experimental results. Finally, the last section of this chapter will address lingering concerns and experimental limitations.

2.1 The Hydrogen Permeation Process

Permeation can be defined as the transfer of a gas from the high pressure side of a solid, non-porous material to the low pressure side of the material [2]. It is also

important to note that permeability strictly refers to the rate of permeation through a solid material and not through pours or holes in the material [2]. The permeation of hydrogen through palladium and palladium alloy membranes is governed by a three step process. The first step is the surface reaction on the upstream side of the membrane where hydrogen molecules adsorb and dissociate on the surface [3,4]. Second, the hydrogen atoms then dissolve into membrane and diffuse towards the downstream side of the membrane [3,4]. Thirdly, the hydrogen atoms recombine at the downstream surface and desorb as hydrogen molecules [3,4]. In order for hydrogen permeation to be successful, it is important that the separation barrier is free of holes or voids that may allow other molecules and/or atoms to pass through the membrane. If such defects are present, then the permeated hydrogen will be contaminated by the presence of these other atoms and/or molecules.

The tendency of hydrogen molecules to dissociate on the surface of palladium has been labeled as a non-activated process [5]. This is not surprising considering the fact that hydrogen permeation through palladium occurs at room temperature and atmospheric pressure. The term non-activated indicates that activation due to an increase in temperature or heat treatment is not required for the dissociation of hydrogen molecules during the adsorption process on the palladium surface. In one study, nanocrystalline powders were investigated for hydrogen storage [6]. The extensive activation procedures required by the nanocrystalline powders were found to be unnecessary with application of a palladium coating. Not only did the palladium coating allow hydrogen dissociation at room temperature, but it also sped up the reaction kinetics and enhanced resistance to air induced impurities [6].

Extensive research in another study revealed that hydrogen dissociation requires a triangular configuration of three or more active sites for hydrogen atoms on the palladium surface [7]. While these details are very general when it comes to the physics governing the dissociation of hydrogen molecules, further specifics will not be addressed in this study.

2.1.1 Modeling the Process

The permeation process is most commonly modeled by Fick's first law as shown below [3,8]:

$$J_H = -D_M \frac{\partial C_H}{\partial x}, \tag{2-1}$$

where J_H is the flux of hydrogen atoms through the membrane, D_M is the diffusion coefficient of the membrane, and C_H is the concentration of hydrogen atoms. From here, it is necessary to relate the hydrogen atom concentration within the membrane to the hydrogen partial pressure using the empirical relation known as Sievert's Law, as shown in Eqn. (2-2) below [3,8].

$$C_H = K_S P_{H_2}^n \tag{2-2}$$

In Eqn. (2-2), the K_S is the Sievert's Constant, and the P_{H2} is the partial pressure of the hydrogen molecules. The partial pressure is raised to the n^{th} power in order to illustrate the dissociation of the hydrogen molecules into hydrogen atoms at the surface of the palladium [3,8]. The n-value is also known as the pressure exponent and varies between 0.5 and 1.0. In order to rewrite Eqn. (2-1) in a more usable form, the partial pressure of hydrogen must be rewritten in terms of the hydrogen activity in solids. The hydrogen activity is defined by the following [3]:

$$a_H = \left(\frac{P_{H_2}}{P^{\circ}_{H_2}}\right)^n \tag{2-3}$$

By rearranging Eqn. (2-3) it is possible to substitute for the partial pressure of hydrogen in terms of the activity in Eqn. (2-2). Further substituting Eqn. (2-2) into Eqn. (2-1) yields the following relation:

$$J_H = -D_M K_S \left(P^{\circ}_{H_2}\right)^n \frac{\partial a_H}{\partial x} \tag{2-4}$$

Now it is necessary to integrate Eqn. (2-4) in terms of membrane thickness, X_M, and the hydrogen activity as shown below:

$$J_H dx = -D_M K_S \left(P^{\circ}_{H_2}\right)^n da_H, \tag{2-5}$$

$$J_H \int_o^{X_M} dx = -D_M K_S \left(P^{\circ}_{H_2}\right)^n \int_{a_H,down}^{a_H,up} da_H, \tag{2-6}$$

$$J_H = D_M K_S \left(P^{\circ}_{H_2}\right)^n \frac{a_H,up - a_H,down}{X_M}, \tag{2-7}$$

where a_H, up is the hydrogen activity just below the upstream surface of the membrane and $a_H, down$ is the hydrogen activity just below the downstream surface of the membrane [3]. Next, Eqn. (2-7) should be rewritten in terms of the partial pressure of hydrogen. By substituting Eqn. (2-3) back into Eqn. (2-7), Fick's law can be rewritten as follows:

$$J_H = D_M K_S \left(\frac{P^n_{H_2},up - P^n_{H_2},down}{X_M}\right), \tag{2-8}$$

where $P^n_{H_2}, \mathrm{up}$ and $P^n_{H_2}, \mathrm{down}$ represent the upstream and downstream hydrogen partial pressures, respectively [3].

2.1.2 Variables That Effect Permeation

Eqn. (2-8) shows how several different variables have an effect on the hydrogen flux, namely temperature, pressure, and membrane thickness. From Eqn. (2-8) it is evident that the hydrogen flux is inversely proportional to the membrane thickness, meaning that the flux will decrease as the membrane thickness increases, and vice versa. The thickness of the membrane only has an effect on the rate of permeation. It does not have any influence on the material's ability to permeate hydrogen [2]. The goal should therefore be to have the thinnest membrane possible. However, this comes with several challenges and will be discussed in greater detail in Section 2.4.

While there is no temperature term present in Eqn. (2-8), both the diffusion coefficient (D) and Sievert's constant (K) vary with temperature [9]. It has also been found that the rate of permeation through solid barriers typically increases at an exponential rate as temperature increases [2,8,10]. In dealing with palladium membranes, researchers have found that the permeability increases at high temperatures because the exothermic hydrogen adsorption on the palladium is dominated by the endothermic activation energy for diffusion [8,11]. Therefore, the flux is directly proportional to the product of D and K, and experiments should be conducted at high temperature.

The pressure difference between the feed and permeate sides of the membrane has a direct impact on the membrane's permeability. A greater pressure difference will result in higher permeability [2,3,8]. In Eqn. (2-8), the difference in the hydrogen partial pressures between the upstream and downstream gases is directly

proportional to the hydrogen flux. Assuming a constant concentration of hydrogen in the feed gas, the partial pressure will increase as the total pressure of the feed gas increases. Simultaneously keeping the total pressure low on the permeate side will increase the pressure difference. If there is a sweep gas present on the permeate side, it needs to be adjusted to a flow such that the hydrogen partial pressure is kept low to maximize the overall pressure difference. When using hydrogen lean mixtures, the best way to increase the pressure difference is by keeping the pressure low on the permeate side and increasing the pressure on the feed side. It is important to remember that there are limitations on pressure, such as the material composition of the membrane, membrane thickness, and the atmosphere within the membrane chamber. These limitations will be discussed further Section 2.4.

2.2 Membrane Development

Palladium has a particular advantage over other materials in its ability to absorb large quantities of hydrogen atoms while still remaining rather malleable [12]. This is compounded by palladium's high hydrogen diffusion rate through the lattice structure [8,10]. These properties make palladium a popular material for producing pure hydrogen as well as separating hydrogen from multi-gas mixtures. While this has been known for several decades, there were many problems faced by researchers during the development of hydrogen separation techniques.

During the mid-1900's, techniques such as passing steam over iron or carbon and electrolysis of aqueous solutions were common methods of capturing hydrogen. Other techniques such as decomposition of hydrogen containing compounds, fractionation of hydrogen containing mixtures, and the use of acids on metals were

popular as well, but many of these processes could not consistently yield high purity hydrogen [2]. Of the few that did produce hydrogen of a high purity, the high price of the equipment and lack of material reliability when compared to the relatively low hydrogen yield made these methods impractical [2,9]. These issues accompanied with the increasing demand for high purity hydrogen lead to more extensive research into the use of palladium as a hydrogen separation barrier.

2.2.1 Pure Palladium Membranes

Researchers quickly found that the use of pure palladium as a separation barrier presented several obstacles. It was determined that under certain conditions palladium experienced an α→β phase transition. This transition occurs at temperatures below 300°C and as the hydrogen concentration is increased [1,8,12,13]. The formation of the β-phase is detrimental to the integrity of the membrane as it has a significantly more expanded lattice structure than the α-phase. The β-phase has the ability to co-exist with the α-phase, growing as more hydrogenation or dehydrogenation cycles are conducted with the membrane at these conditions [1,12,13]. As the β-phase expands, it can cause severe strains in the palladium. This can lead to defects in the membrane such as material distortion or fracture [1,8,12,13].

The recommended technique to overcome the α→β phase transition during hydrogenation or dehydrogenation cycles is to operate the palladium membrane in the single phase region of the Pressure-Composition-Temperature diagram, which is shown in Figure 2-1 below [1,12]. As can be seen, the best way to preserve the life of the membrane is by keeping the membrane in the α-phase using an operating

temperature above 300°C. One key ingredient to this formula for success to remember is that even after hydrogen separation operations are complete the membrane could still be in a hydrogen environment. If the membrane is allowed to cool in a hydrogen environment, the palladium could still experience an α→β phase transition [1,12]. It is best to avoid this by ensuring the hydrogen has been flushed from the system prior to allowing the palladium membrane to cool [1]. To be on the safe side, it is also a good idea to heat the membrane to its desired temperature in an inert environment.

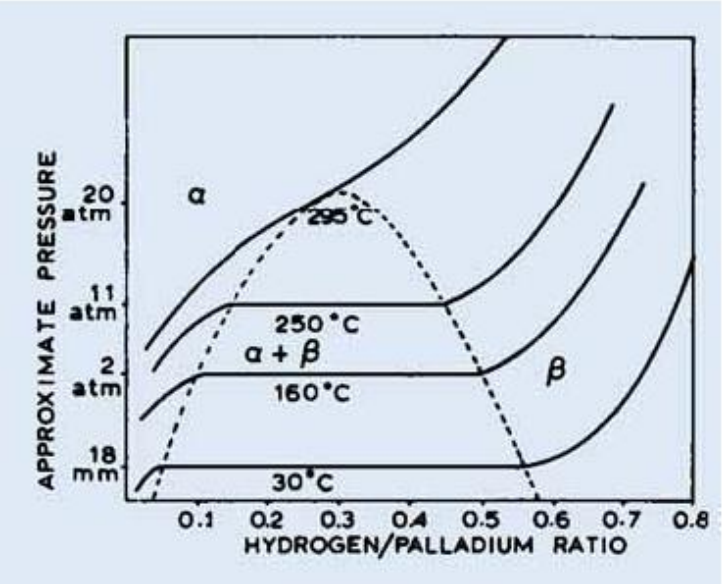

FIGURE 2-1. Relationship between hydrogen absorption in palladium and temperature [12].

Another challenge in using pure palladium membranes is the material's strength. Even at temperatures where the palladium won't undergo an α→β phase transition there is still a risk of fracture. As pointed out at the beginning of this chapter, the pressure difference is the driving force for the flux calculation. The higher the pressure on the feed side of the membrane, the greater the flux. However,

a thicker palladium membrane is required in order to withstand higher pressures [4,14]. It is already known that the hydrogen flux is inversely proportional to the membrane thickness, as was shown in Eqn. (2-8). While increasing the pressure increases the flux, it also calls for a greater membrane thickness which in turn decreases the flux [4,14]. This imposed a constant battle for researchers and led to the search for better separation barriers. One such method explored was the use of palladium alloyed with other metals.

2.2.2 Pd-Ag, Pd-Au, and Pd-Cu Alloy Membranes

Researchers began looking for different palladium alloys to enhance hydrogen permeability while also helping to overcome the shortfalls associated with pure palladium. This began when Dr. James B. Hunter discovered that using a palladium-silver alloy achieved better permeation results than pure palladium [2]. His experiments were conducted at various temperatures and pressures and then compared to permeation data for pure palladium. Dr. Hunter's early experiments indicated that using a Pd-Ag alloy comprised of 10-50% weight silver were preferred to other Pd-Ag compositions and pure Pd [2]. Narrowing the range even further, Dr. Hunter found that even more favorable results were yielded when using Pd-Ag membranes with 20-40% silver composition [2].

Following Dr. Hunter's studies, others began to test various compositions of Pd-Ag membranes. U.S. Patent No. 3,247,648 to McKinley states that high concentrations of silver in palladium can cause severe degradation in the membrane's structural integrity when exposed to hydrogen [9]. McKinley reveals that a high silver content expands much more than the palladium contained within the membrane

upon the introduction of hydrogen [9]. With this knowledge, it can be stated that fractures are more common in membranes containing a high percentage of silver. It is also important to note that these fractures are a result of hydrogen exposure rather than temperature changes [9]. McKinley wished to further test membranes across similar ranges as Hunter while also testing palladium membranes alloyed with metals other than silver – such as Pd-Cu, Pd-Au, and Pd-Ni. He found that the Pd-Ag membranes he tested containing over 40% silver performed with similar results as were stated by Dr. Hunter [9]. Table 2-1 below shows the results of McKinley's various tests of pure palladium and palladium alloy membranes. One thing McKinley found that differed from Hunter's results was that the Pd-Ag membrane with 10% silver performed better than the Pd-Ag membrane with 27% silver at 300 psig upstream and 350 degrees Celsius. At 75 psig upstream and 350 degrees Celsius, the Pd-Ag membrane with 27% silver still yielded the highest permeation [9]. It's also important to note that McKinley found that a Pd-Cu membrane with 40% copper had the 3rd best permeation rate at both 75 psig and 300 psig.

Run No.	Barrier foil composition (wt. percent)		Barrier foil thickness, mils		Permeability			
					Hydrogen transfer rate at 75 p.s.i.g. upstream pressure—0 p.s.i.g. downstream pressure		Hydrogen transfer rate at 300 p.s.i.g. upstream pressure—0 p.s.i.g. downstream pressure	
	Nominal	Actual	Nominal	Actual	Measured (s.c.f.h.)	(S.c.f.h.)(Mil) / (Sq. Ft.)	Measured (s.c.f.h.)	(S.c.f.h.)(Mil) / (Sq. Ft.)
7	100% Pd	100% Pd	1	1.12	0.142	55	0.433	167
14	10% Ag-90% Pd	10.29% Ag-90.00% Pd	1	1.05	0.260	94	0.811	294
14 Repeat	10% Ag-90% Pd	10.64% Ag-89.36% Pd	1	1.03	0.23+	82+		
1	27% Ag-73% Pd	27.18% Ag-73.05% Pd	1	0.92	0.298	95	0.757	240
13	40% Ag-60% Pd	40.05% Ag-59.97% Pd	1	0.93	0.113	36	0.254	82
12	52% Ag-48% Pd	52.30% Ag-47.91% Pd	1	1.24	0.012	5.1	0.027	11.6
11	80% Ag-20%Pd	80.25% Ag-20.09% Pd	1	1.05	0.000	0	0.000	0
6	5% Au-95% Pd	4.9% Au-93.7% Pd	1	1.01	0.184	64	0.514	179
2	20% Au-80% Pd	20.3% Au-78.1% Pd	1	1.02	0.159	56	0.462	162
5	40% Au-60% Pd	39.7% Au-60.6% Pd	1	0.90	0.082	25.4	0.229	71
4	55% Au-45% Pd	54.6% Au-44.8% Pd	1	1.00	0.017	5.9	0.046	15.9
3	0.5% B-99.5% Pd	0.5% B-99.5% Pd	3	2.87	0.058	57	0.161	159
8	10% Cu-90% Pd	9.8% Cu-90.1% Pd	1	0.97	0.093	31	0.246	82
9	40% Cu-60% Pd	38.7 Cu-60.1% Pd	1	1.03	0.208	74	0.506	180
10	10% Ni-90% Pd	9.8% Ni-90.6% Pd	1	1.05	0.034	12.3	0.089	32

TABLE 2-1. The above table shows McKinley's permeation test results. The permeation data was measured in standard cubic feet per hour (scfh) [9].

The early success of Pd-Ag membranes led to significant study of alloying palladium with other Group I-B metals such as gold and copper. McKinley was one of the first to report increased permeability through use of these other metals. Using Pd-Au alloys was found to reduce poisoning on the membrane caused by feed gases containing sulfur [12]. However, Pd-Au membranes never seemed to become as widely used as Pd-Ag and Pd-Cu membranes.

Additions of copper to palladium initially reduces permeability at lower levels, but then increases dramatically around 40% copper content [12]. Studies revealed that hydrogen permeation is significantly higher in body-centered cubic (BCC) metals than face-centered cubic (FCC) metals [10]. Upon alloying palladium with copper, a BCC β-phase forms and promotes greater hydrogen transport. It was found that the addition of copper to palladium yielded a diffusion coefficient two orders of magnitude greater than pure palladium at room temperature [12]. However, Pd-Cu alloys also demonstrate much lower hydrogen solubility. The high diffusion coefficient is therefore offset by a lower concentration gradient, limiting Pd-Cu alloys

to permeation rates barely exceeding those of pure palladium [12]. Several attempts have been made to add other elements to palladium, but they've mostly been met with less than desirable results. Some of these metals include platinum, iron, chromium, nickel, and ruthenium [12]. In addition to the aforementioned metals, some of the rare earth metals have been found to perform well when alloyed with palladium.

2.2.3 Rare-Earth Palladium Alloys

Rare-earth metals offer further possibilities for palladium alloy membranes. Initial studies by I.R. Harris and M. Norman and also by J.R. Thompson yielded rare earth metal solubility values in palladium [15]. They discovered that cerium, yttrium, gadolinium and thorium were soluble in palladium while lanthanum and praseodymium were relatively insoluble [15]. The solubility limit values for these metals were 12 percent for cerium, 12 percent for yttrium, 11 percent for gadolinium, and 16 percent for thorium. Figure 2-2 below shows the increase in lattice spacing at room temperature for several palladium alloys. It is evident that the rare earth metals create larger spacing than silver. The primary reason for this is the fact that yttrium, cerium and gadolinium atoms are roughly 30 percent larger than palladium atoms. As a result, rare earth-palladium alloys can achieve a higher hydrogen solubility gradient within the membrane, thus increasing the hydrogen permeation rate [1,15].

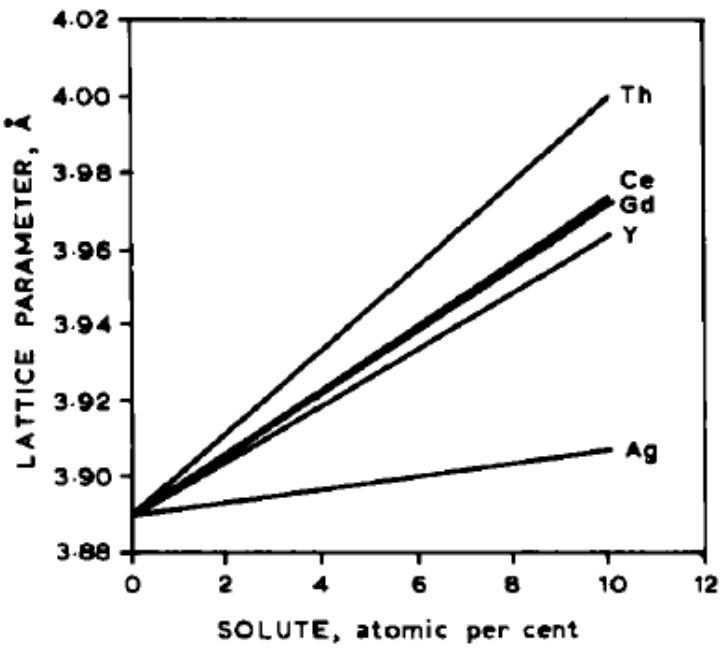

FIGURE 2-2. Rare earth metals increase the lattice spacing between atoms at room temperature significantly when alloyed with palladium compared to noble metals [15].

While the diffusion coefficients are relatively similar for palladium-silver, palladium-cerium, and palladium-yttrium, their concentration gradients vary due to the difference in hydrogen solubility [1]. Figure 2-3 below shows Knapton's results of testing two compositions of palladium-cerium compared to palladium-silver at 300 psig and up to 500 degrees Celsius. The two compositions of palladium-cerium were 7.7% and 12.7% cerium in palladium. The palladium-silver membrane consisted of 23% silver in palladium. The hydrogen flux of the 7.7% cerium alloy was found to be roughly 25% lower than that of the 23% silver alloy at higher temperatures [1]. The hydrogen flux through the 12.7% cerium alloy tended to drop off above roughly 350 degrees Celsius.

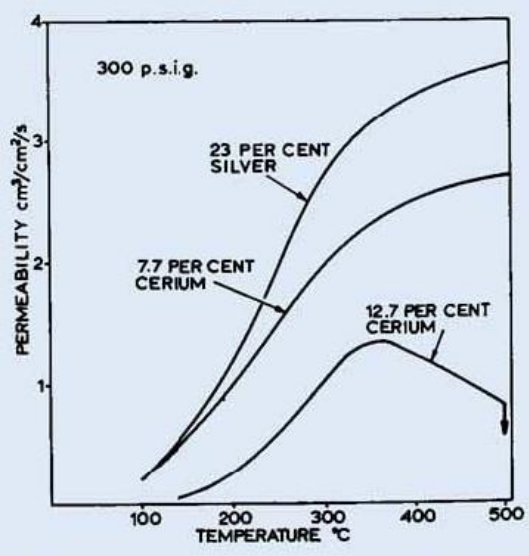

FIGURE 2-3. This figure relates the permeabilities of two rare earth-palladium alloys with Pd-Ag at constant pressure and varying temperature [1].

2.2.4 Refractory Metal Membranes

Around the same time McKinley was doing his studies, Makrides et al. were experimenting with palladium alloy membranes that differed from what had been used by both Hunter and McKinley [2,4,9]. Makrides et al. pursued other alloys due to shortcomings associated with the use of palladium and palladium-silver membranes – such as high cost, relatively short operational lifetime, low rates of hydrogen production, and in some cases failure to sustain high pressure differentials [4].

Makrides et al. decided to focus their experiments on the study of using substitute metals that would favor hydrogen permeation through their lattice structures. They were able to determine that Group V-B metals – vanadium (V), niobium (Nb), and tantalum (Ta) – are capable of absorbing more hydrogen, thus leading to a higher concentration gradient than palladium with a lower diffusion

coefficient [4]. At first glance, these new membranes seemed to have many advantages over Pd and Pd-Ag membranes – they cost less, had greater tensile strength, and displayed better permeability in the 400-500 degrees Celsius range at the same pressure gradient [4]. However, Makrides et al. began to see that the Group V-B metals were subject to the formation of an oxide surface film that greatly decreased the permeability [4].

It was further found that this film could be removed by heating the membrane in a vacuum, but it would form again once the membrane was put back in use at lower temperatures [4]. As a result, Makrides et al. determined that the use of Group V-B metals alone didn't offer a better method of hydrogen separation. U.S. Patent No. 3,350,846 to Makrides et al. describes the process by which they prepared a tantalum membrane with a thin palladium coating [4]. A cross-sectional schematic of their membrane can be seen below in Figure 2-4. The thin Pd coating prevented the formation of any oxides and thus preserved the permeability of the membrane [4].

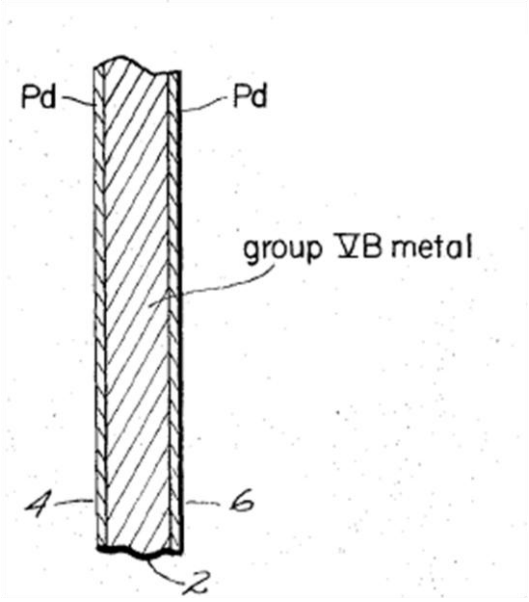

FIGURE 2-4. The above figure depicts a schematic of a Group V-B membrane constructed by Makrides et al.. coated with palladium [4].

At the time Makrides et al. were conducting their studies, the general rule of thumb for minimum membrane thickness was 1 mil. It is important to note that, as time progressed, membrane fabrication techniques evolved to allow for the development of thin membranes on the order of microns. As was stated previously, the flux is inversely proportional to membrane thickness. Therefore, there was a strong desire to make a very thin membrane without sacrificing its ability to withstand the high pressures it would encounter in commercial application [4]. U.S. Patent No. #3,350,846 to Makrides et al. describes an experiment using three different membranes [4]. Each membrane consisted of a different Group V-B metal of varying thickness and a Pd coating of roughly 0.1 microns. At the time, Pd thicknesses less than 0.01 microns were subject to pinhole leaks and thicknesses greater than 0.1 microns were too costly [4]. The permeation data can be seen below in Table 2-2.

Membrane A consisted of 8 mils of tantalum, membrane B consisted of 5 mils of niobium, and membrane C consisted of 10 mils of vanadium [4]. Each test was conducted at relatively low pressure and high temperature.

In the end, Makrides et al. concluded that all three membranes were more ductile and had higher tensile strengths than Pd and Pd-Ag membranes [4]. They also stated that their membranes yielded higher permeation rates across the preferred temperatures of operation than Pd and Pd-Ag membranes that had been tested by others [4]. However, they encountered a problem with their membranes becoming brittle after repeated cycles due to hydrogen absorption in the lattice structure of the metals. It was determined this could be overcome by ensuring the membranes were cooled in a hydrogen free environment [4]. It is important to note that Table 2-2 clearly shows the tests were conducted at relatively low pressures. While Makrides et al. stated the Group V-B metals displayed greater tensile strength than Pd and Pd-Ag, their results do not show any tests conducted in the higher pressure ranges that McKinley used for his experiments.

Membrane	Pressure Differential (mm. Hg)	Membrane Temperature (° C.)	Permeability (cc./sec./cm²)
A	484	400	.084
	484	500	.101
	256	400	.051
	256	500	.066
	144	400	.017
	144	500	.042
B	484	400	.158
	256	500	.108
	144	500	.074
C	230	550	.026
	138	550	.016

TABLE 2-2. This table shows permeation data for three different membranes developed by Makrides et al. Membrane A was made of tantalum, membrane B of niobium, and membrane C of vanadium. Each membrane had a thin palladium coating on each side [4].

Decades later, further studies revealed more information about the Group V-B metals as hydrogen diffusion barriers. It became apparent that the arrangement of the crystalline structure within the metals played a significant role in hydrogen transport. Several reasons influenced further study into the use of refractory metals in the construction of composite membranes. Greater permeability is expected as a result of the BCC crystalline structure in refractory metals. While known for their tendency to become brittle in a hydrogen atmosphere, as was discussed previously, this can be overcome by adding a thin coat of palladium on both sides. Higher permeation rates allow for a thicker membrane, which means increased structural stability over FCC counterparts while still yielding a higher hydrogen flux. [10]. Another advantage of using refractory metals in composite membranes is they cost much less than using pure palladium or palladium alloy membranes [10].

There are some distinct disadvantages to using refractory metals. For one, the surface oxide layer that forms on the refractory metal must be removed before the application of the palladium coating [10]. The quality of the palladium coating is also of concern. It must be free from contaminants and pinholes in order to be effective [10]. Ion milling using argon was used to cleanse the surface of the tantalum in a vacuum chamber. By using ion-beam sputtering to coat tantalum with a thin layer of palladium, Peachey et al. attempted to neutralize the surface layer oxides [10]. They also prepared a tantalum membrane using just acetone as a cleaning agent prior to application of the palladium coating. Figure 2-5 below displays the difference between the two preparation methods. The squares represent the tantalum membrane prepared using ion milling. The X's represent the tantalum membrane prepared without the ion milling. It is evident from the plot that surface cleaning prior to coating with palladium improves the permeability of the composite membrane. Since this method runs the risk of introducing impurities between the cleaning and application processes, Peachey et al. negated this problem by conducting both operations in a single sealed vacuum chamber [10].

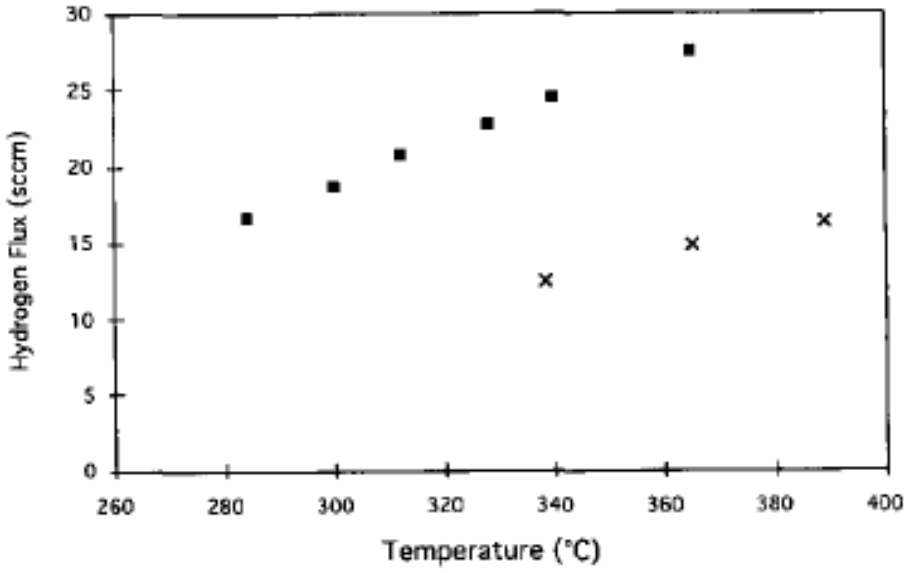

FIGURE 2-5. The above figure shows the significance of cleaning the refractory metal prior to application of the palladium coating. The squares represent the Ta membrane cleaned using ion milling and the X's represent the Ta membrane prepared without the ion milling. The flux is measured in standard cubic centimeters [10].

2.3 Membrane Housings and Experimental Setups

Design and fabrication of a membrane for use as a hydrogen diffusion barrier wouldn't be complete without a housing in which to seat the membrane. The housing is an integral part of the process and must be designed carefully to accommodate the membrane. The membrane is the only barrier between the feed gas and the permeate gas. The housing must be able to provide a good seal around the membrane to prevent leakage. In addition, the casing must be able to withstand elevated pressure and temperature. Careful consideration must be given to these factors when designing the membrane housing.

Just as the housing is pivotal for membrane operation, the experimental setup must be designed to accommodate both the membrane and the membrane casing. The

experimental setup incorporates the membrane and its housing with everything else that will be needed to construct a hydrogen separation facility. Examples of other things to consider are temperature and pressure reading instruments, gas sources and lines, flowmeters and flow controllers, a heat source, and a method to analyze the gas. Throughout this section, several examples of membrane housings and facilities will be presented in detail.

2.3.1 Membrane Casing Development

An early example of a membrane housing designed for hydrogen separation is the one developed by Makrides et al. in the 1960's [4]. The casing in which they tested their membranes can be viewed schematically below in Figure 2-6. The feed gas inlet is at the left side of the figure (18) whereas the permeate outlet is at the right side of the schematic (20). The Group V-B metal membrane (10) used by Makrides and his colleagues is located at the right side of the narrow inner tube (12). The membrane was securely placed in the end of the stainless steel tube using electron beam welding to create a leak-proof diffusion barrier [4]. The valve (24) on the bottom of the diagram served as an outlet for non-permeated gas as well as a way to regulate pressure and control the flow [4]. The pressure gradient across the membrane was maintained through either the use of a pump on the permeate side or the presence of a high pressure gas on the feed side. The casing was designed to be used at high temperature with an electrical heating unit (26), but it was also possible to forgo the use of a heating element if the incoming gas was already at an elevated temperature. The gas would then heat the casing via convection heat transfer [4].

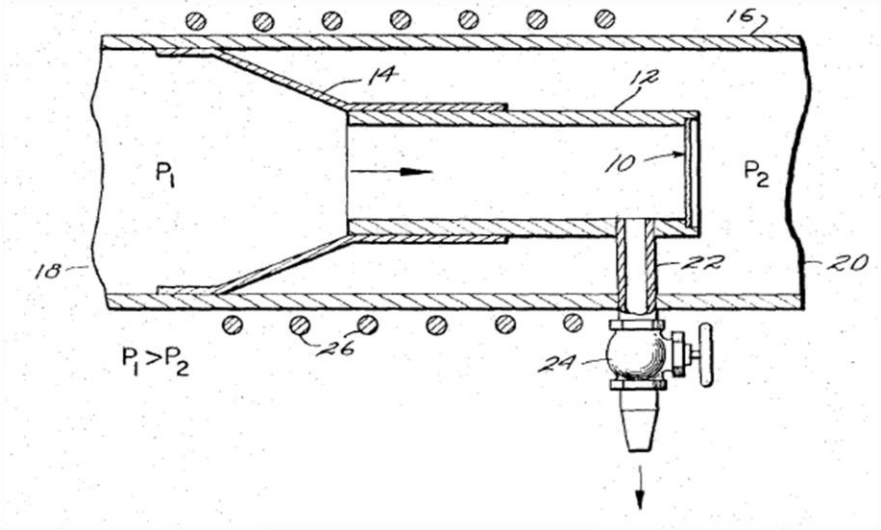

FIGURE 2-6. This schematic depicts the membrane housing used by Makrides and his colleagues to test their Group V-B metal composite membranes. A pressure gradient across the membrane was maintained by keeping a very high pressure at the inlet (P_1) or by using a pump on the permeate side to keep the pressure low (P_2) [4].

Although the casing in Figure 2-6 was designed a half century ago, it provided a basis on which future casings could be constructed. Others began to construct similar housings; some of these designs were for tubular membranes and others incorporated disk membranes. Figure 2-7 below shows examples of both. The addition of a sweep gas became more and more common for experimental use. The use of a sweep gas alleviated the need for a pump on the permeate side or extremely high pressures on the feed side. The sweep gas prevented the build-up of hydrogen on the permeate side [5,16]. A hydrogen build-up on the permeate side would lower the hydrogen partial pressure difference between the two sides. Since pressure is the driving force, this would decrease the permeation rate. The use of a sweep gas also enables a large hydrogen partial pressure difference while lowering the total pressure difference. This is especially important for membranes that lack high mechanical

strength. The inert gases nitrogen and argon are most commonly used as sweep gases while the use of steam is another possibility. Steam is the easiest to separate from hydrogen through condensation.

Figure 2-7 below displays two schematics of casings used for hydrogen separation. The casing shown in Figure 2-7(a) houses a tubular Pd membrane supported by a porous glass tube. The feed gas enters from the bottom right side and flows around the outside of the tube, whereas the sweep gas enters at the top and flows through the inside of the tube [17]. The hydrogen permeates through the palladium and the glass tube to the inner tube where it is carried out of the casing by the sweep gas. The casing shown in Figure 2-7(b) displays a diagram of the housing used for a Pd-Cu membrane disk. The membrane creates a diffusion barrier between the feed side at the left and the permeate side at the right [16]. As in (a), the hydrogen permeates through the membrane and is carried out of the casing by the argon sweep gas. While both of the schematics in Figure 2-7 show the inclusion of a sweep gas, it is still possible to separate hydrogen without its use. In the case of Figure 2-7(a), the sweep gas was used in order to heat the membrane in an inert medium, but it wasn't necessarily used during experiments [17].

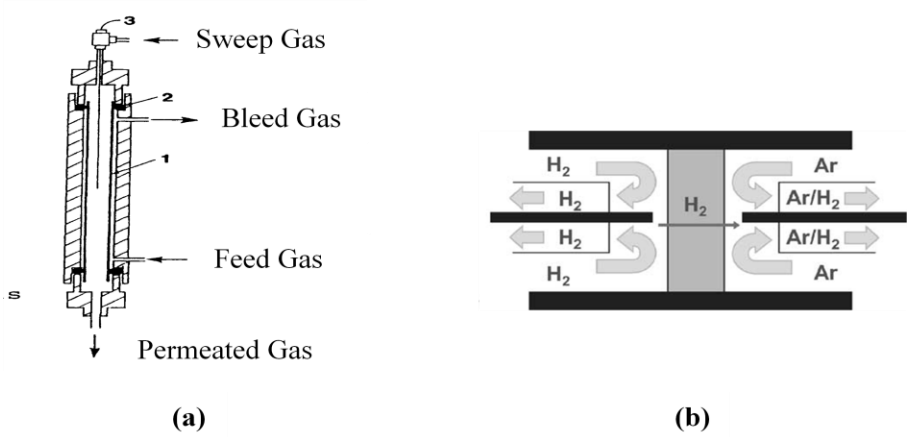

FIGURE 2-7. Schematic diagrams of two membrane housing examples. The housing in (a) is for a tubular membrane while (b) is for a membrane disk. Both designs incorporate the use of a sweep gas [16,17].

Casing assembly around the membrane is pivotal in attaining a leak-free diffusion barrier. If leaks are present around the membrane the permeated hydrogen has the possibility of being contaminated by non-permeated gas. While some leaks may not be present at standard conditions, they may arise as the temperature and pressure increase. Careful consideration must therefore be taken to ensure that the seals are maintained throughout the experimental range. For Ilias and colleagues, the use of a stainless-steel housing early in their studies suffered from leakage at high temperatures [11]. To overcome this problem they acquired a casing that would self-seal at high temperatures through the use of graphite and copper seals as can be seen in Figure 2-8 [11]. The outer shell of the casing in Figure 2-8 was made of stainless steel (AISI 310) whereas the inner parts were made of titanium. The graphite seals were used against the ceramic edges of their membrane while the copper seals were placed between the stainless steel tubes [11]. Ilias et al. reported that there was no external detection of hydrogen as a result of using this assembly [11].

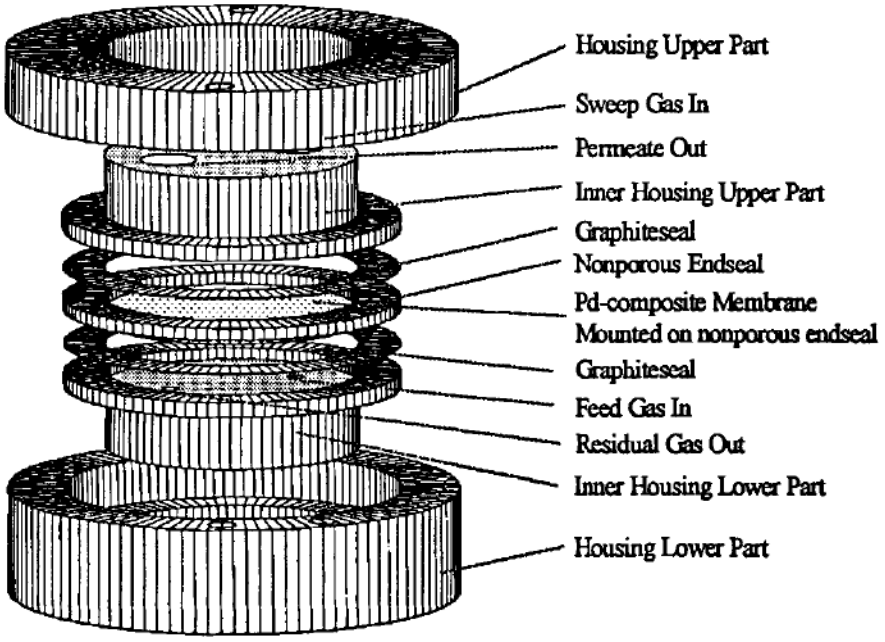

FIGURE 2-8. Schematic of a self-sealing (at high temperatures) membrane housing. This cell was designed by the Velterop Ceramic Membrane Company of the Netherlands, Model LTC Type K-500 [11].

An example of a membrane casing assembly used by Howard et al. is illustrated below in Figure 2-9 [16]. Their Pd-Cu membrane was placed between a nickel alloy washer and a porous support. The porous support was mounted on the permeate side in order to protect the membrane from potential failure from a pressure gradient at high temperatures [16]. The membrane surface was in contact with the support, but the two were not attached by any means. The casing and membrane were held together using TIG welding and brazing techniques developed by the U.S. Department of Energy's (DOE) National Energy Technology Laboratory [16]. These methods were used in order to assure there was no damage to the membrane as a result of the extreme heat associated with welding operations [16].

The assembly on either side of the membrane consisted of an inner tube and an outer tube. The sweep and feed gases flowed between the inner and outer tubes where they would then contact the membrane and exit through the inner tubes as illustrated in Figure 2-7(b) [16]. The design features of this particular assembly allowed for high operating parameters. The casing was capable of functioning at temperatures up to 1173 K and pressures up to 450 psi [16].

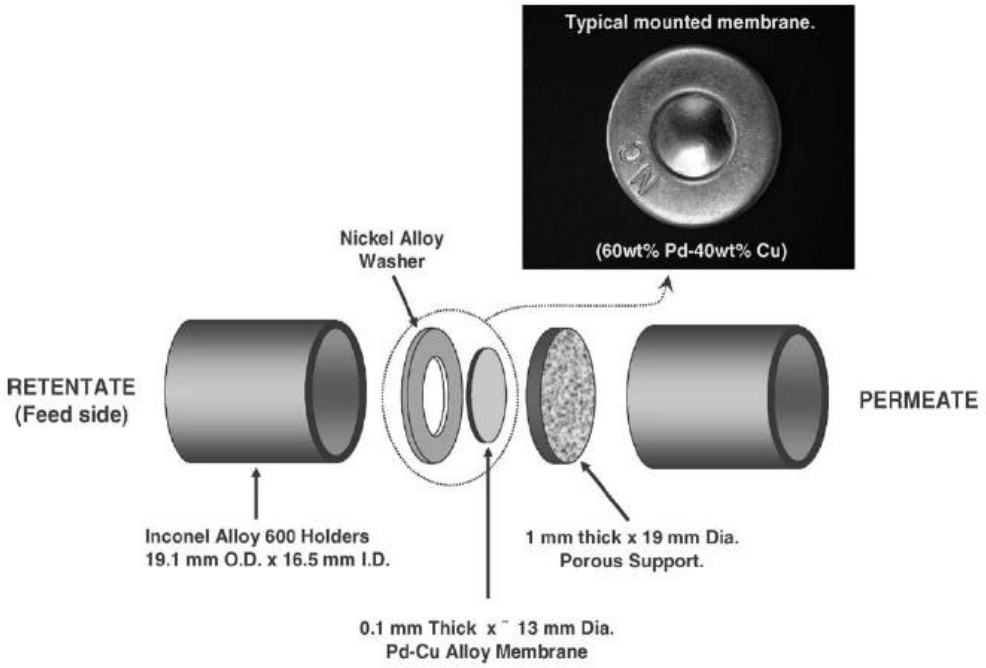

FIGURE 2-9. Housing assembly for a Pd-Cu membrane [16].

Gas leakage and membrane distortion are primary concerns when running hydrogen separation experiments. It is important that the membrane housing used in the experiments addresses both of these issues. The casing needs to be able to withstand the desired operating parameters. High temperatures and pressures can increase the chances of experiencing leaks or damaging the membrane. Using materials that can withstand high temperatures to act as a sealing surface is essential

in preventing leaks. The presence of a pressure gradient between the permeate and feed sides of the membrane calls for the use of a porous media – whether part of the membrane or not – to negate the potential for membrane distortion. The placing of the membrane and the housing assembly needs to be completed in such a way that it does not damage the membrane from exposure to extreme heat or excessive force. Access to the membrane may be limited depending on membrane mounting and casing assembly methods. This must be considered when designing the casing if it is anticipated that multiple membranes may be used over time.

2.3.2 Experimental Setup

Once the membrane has been fabricated and a casing has been built to house it, the next step is building a setup to run experiments. The setup, or experimental facility, incorporates everything else that will be needed and includes, but is not limited to, the following: gas lines to deliver and remove gases from the membrane housing, pressure gauges, flowmeters or flow controllers, valves, thermocouples, a heating method, gas sources, a gas sampling/analyzing method, and a gas exhaust system. Two examples of experimental setups are provided below.

The membrane casing designed by Ilias et al. described in the previous section was integrated in the facility illustrated by Figure 2-10 below [11]. The feed gas (yellow) and sweep gas (red) routes can be seen as highlighted. Ilias and colleagues used stainless steel tubes for their gas lines with the diffusion cell mounted in a tubular furnace (Lindberg Type 55347) [11]. As can be seen in Figure 2-10, flowmeters were used at the inlet and rotameters after the diffusion cell in order to record the mass flow rates for the gas streams. They monitored the system pressure

with pressure gauges and used valves and a pressure transducer to make adjustments in the pressure. Samples were taken from various sample ports (green arrows) using a syringe and were analyzed using a Gas Chromatograph (GC) (Perkin-Elmer Sigma 2000) [11]. This type of setup is relatively similar to what other researchers have used. The use of multiple sample ports is advantageous in allowing the experimenter(s) to test the gas composition at several stages of the process. One disadvantage, however, is that there are no direct connections to the GC for sampling. The use of direct sampling lines would help speed up the sampling process.

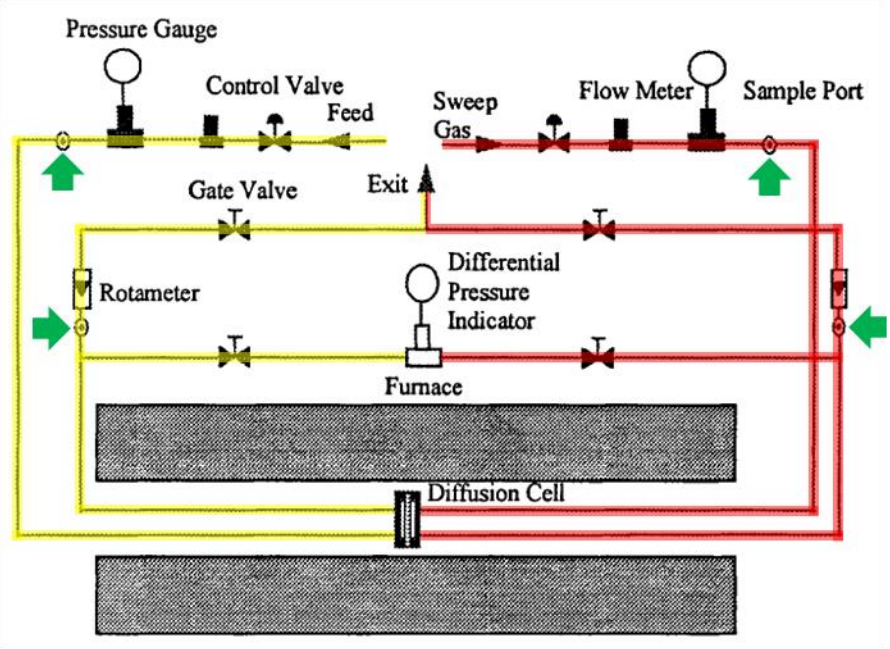

FIGURE 2-10. Experimental facility for hydrogen separation [11]. The yellow lines highlight the feed side, the red lines highlight the sweep side and the green arrows indicate sample ports.

The facility depicted by Figure 2-10 is an example of a pretty standard setup used by researchers. In some cases, the experimental objectives require much more sophisticated facilities. An example of this is illustrated in Figure 2-11 below. Methane steam reforming has long been a technique used to produce hydrogen.

Gielens et al. focused their studies on using membranes to remove hydrogen during the steam reforming process [18]. They designed their setup to study the effects of CO_2 and steam on the hydrogen flux through pure Pd and Pd-Ag membranes. Their main concern was to understand the influence that carbon dioxide and steam would have on the surface of the membrane, specifically whether or not they would impede the dissociation of hydrogen at the surface [18]. Figure 2-11 shows water was added to the feed gas and heated to form steam, then cooled again after passing over the membrane.

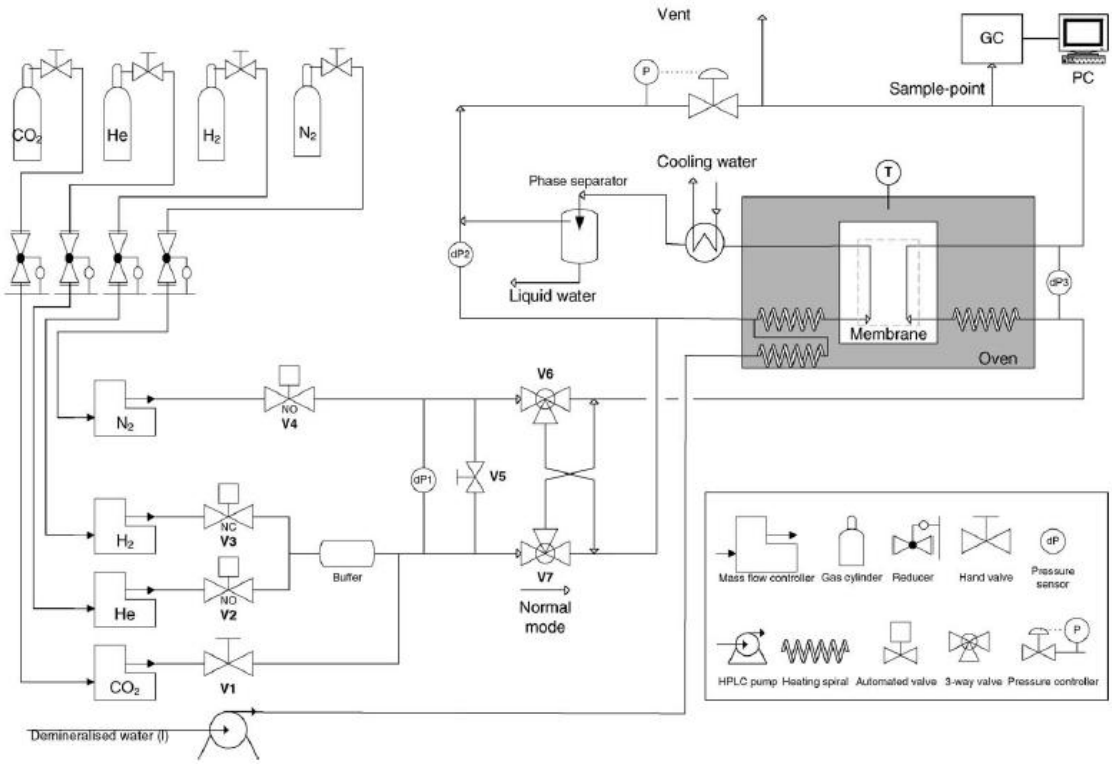

FIGURE 2-11. Experimental facility for the study of the effects of CO_2 and steam on the hydrogen separation process [18].

Various designs can be found in the literature with each one having relatively the same basic design concept. There are apparent similarities between the two facilities shown in Figures 2-10 and 2-11. However, they each have their own unique

characteristics. Understanding the experimental objectives is important in constructing the facility. As these goals may change over time, the setup may require alterations to support the new objectives. Researchers must consider this possibility in the early stages. This will ensure the construction of a flexible setup that can be easily updated. If the setup is designed with too much emphasis on the initial experiments, then modification might not be possible and a new facility may have to be assembled if the outlook changes.

2.4 Experimental Membrane Limitations

2.4.1 Design Constraints

Certain limitations result directly from parameters within Fick's Law while others are related to the mechanics of the membrane. Often times these limitations are related, whether directly or inversely. Membrane composition and construction is pivotal in determining the challenges which will be faced by researchers. Of the types of membranes that have been mentioned in this chapter not one can be considered ideal. When trying to decide which ones are better than others, it is important to remember the limitations associated with each. The researcher should choose the membrane that he or she feels will best meet the requirements for his or her project.

Fick's law states that the membrane permeation rate increases as the membrane thickness decreases. As a membrane's thickness lessens there is a greater likeliness of problems arising. If the membrane is made too thin it is more likely that small pinholes will form during the membrane preparation process [2]. Another problem is the structural integrity of the membrane. The thinner the membrane, the

more susceptible it is to structural degradation, whether it be from exposure or high pressure feed streams [4,9]. The mechanical strength of a membrane is usually determined experimentally since several factors make it tough to estimate. It is dependent on material properties, the fabrication method and the thickness [19]. The thickness problem can be partially alleviated by use of membranes with greater mechanical strength, such as palladium alloyed with other metals. However, there will always be a thickness limitation. Pure palladium membranes, for example, have primarily fallen within the 10 to 1000 micron thickness range [5]. Even the use of a porous support will not prevent failure of a thin membrane, although the use of supported Pd and Pd composite membrane layers with thicknesses less than 10 microns have been reported [20,21,22] The membrane support can be assumed to have much greater strength than that of the membrane, so the membrane's strength still remains the limiting factor.

Temperature and pressure pose just as many challenges as membrane thickness and are in fact closely related. An expression has been derived by Van Rijn et al. [23] to estimate the maximum pressure that can be applied to a thin ductile membrane.

$$P_{max} = 6.4 \frac{X_m \sigma_{yield}^{3/2}}{l E_y^{1/2}} \tag{2-9}$$

In Eq. (2-9), x_m is the membrane thickness, σ_{yield} is the yield stress, l is the length of membrane's shortest side and E_y is Young's modulus [19]. It is well known that the yield stress and Young's modulus are temperature dependent. Fick's law states that the greater the hydrogen partial pressure difference between two sides of the membrane, the greater the permeation rate. Eq. (2-9) takes three factors – thickness,

temperature, and pressure – into consideration. It allows for predictions of the maximum pressure based on material selection, thickness, and operating temperature and can be a useful tool during the design process. Knowing the desired operating conditions ahead of time will allow for appropriate selection of material and thickness to maximize hydrogen permeation.

2.4.2 Hydrogen Separation Facility

Most of the challenges with the system design are a result of the membrane as was stated in the previous section. However, the overall system can present limitations as well. Pressure build-up on the permeate side of the membrane will decrease the hydrogen partial pressure gradient across the membrane and consequently lower the permeation rate. Allowing for free flow, venting or continuous sampling on the permeate side will help prevent this. Using a sweep gas will prevent the hydrogen concentration from building up on the permeate side, and it also has the benefit of protecting the membrane from mechanical failure. There have been some instances of membrane deformation due to a large pressure drop [5]. There are several factors that determine when a membrane will fail due to pressure, as was highlighted by Eq. (2-9).

The use of a sweep gas can help prevent membrane distortion, but it will be at the expense of the permeation rate. A drawback to using a sweep gas, such as argon or helium, is that it is purely for experimental use. It provides an economical way to study the permeation rate and the factors that influence it through the use of various membranes. Steam is another possible sweep gas candidate, but is not as common in experiments. This is most likely due to the added complications and expense that

result from incorporating steam into the hydrogen separation system. Control devices within the system can also have an effect on the permeation rate. The use of flowmeters, flow controllers, or rotameters can restrict flow either before or after the membrane. It is important to choose all measuring and controlling devices such that the desired flow can be attained accurately.

2.5 Feed Stream Impurities

Several studies have been conducted over the years to determine the extent of the effects impurities in the feed gas have on hydrogen permeation. It is of great concern that impurities in the feed gas can lead to membrane decomposition or decreased permeation fluxes. These impurities tend to consist mostly of other gases such as N_2, CO, CO_2, CH_4 and H_2O. It is no coincidence that the aforementioned gases are of interest considering many of them will be found in practical hydrogen separation feed gases. Understanding how these gases will influence both hydrogen permeation and membrane sustainability could lead to building more dependable membranes and effecting better permeation techniques. To do so, engineers have conducted experiments over a wide range of parameters on membranes of varying composition. Their results will be discussed in this section.

2.5.1 Nitrogen

A study conducted by Wang and colleagues employed the use of a thin Pd membrane mounted on corundum (α-Al_2O_3) and subjected to three feed streams: N_2, H_2, and an H_2/N_2 mixture [24]. The H_2/N_2 mixture was kept at a 1:1 molar ratio and a sweep gas was not used in an effort to attain pure hydrogen. Their membrane was

sealed in a self-made housing and tested at pressure differences up to 29 psi at room temperature and in the 350-450 degrees Celsius range [24]. During pressure testing, it was found that there was some flux of N_2 present on the permeate side, but this value was minuscule compared to the hydrogen flux. Initially it was assumed that the N_2 flux was a result of Knudsen diffusion through cracks in the Pd layer [24]. However, this was ruled out when the N_2 flux remained constant as temperature increased. If the N_2 presence was due to Knudsen diffusion, the flux would have decreased with increasing temperature [24]. Further inspection of the membrane through an SEM image determined that the membrane layer was intact and thus it was concluded the leaks were a result of faulty seals.

Initial experiments on a newly prepared membrane were conducted with the use of pure gas feed streams. The membranes were exposed to H_2, N_2, and H_2, sequentially, for varying time periods. The results of the experiments by Wang et al. can be seen in Figure 2-12 below [24]. The membranes were subjected to a hydrogen atmosphere for the first 1000 (1) minutes, with the first permeation measurement at the 120^{th} minute. The membranes were then subjected to a nitrogen feed stream for the 1000-1230 (2) minute time frame. In the last time interval, the membranes were exposed to a hydrogen atmosphere again for the 1230-2640 (3) minute period. During period (1), the membranes showed an increasing flux over time until it steadied out around the 1000^{th} minute. At this point they switched to stage (2) where they applied a pure nitrogen stream to the membrane for 230 minutes. The nitrogen levels remained constant during this time period and were similar to the original test

values [24]. This led Wang and colleagues to believe that there was no membrane deterioration as a result of hydrogen exposure during stage (1) [24].

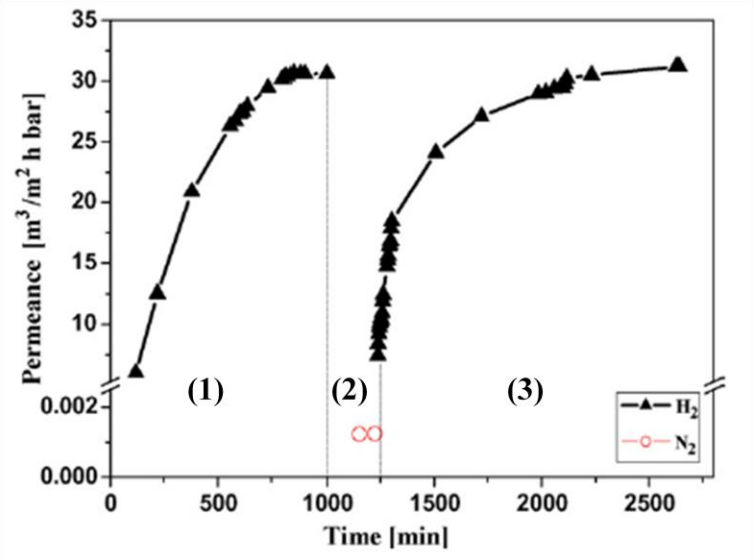

FIGURE 2-12. Permeation differences vs. time resulting from a varying feed stream of hydrogen (0-1000 min), nitrogen (1000-1230 min) and hydrogen (1230-2640 min) at 550 degrees Celsius [24].

The hydrogen permeance levels at the start of stage (3) of the experiments yielded much lower values than at the end of stage (1). In addition, it took much longer, roughly 800 minutes, for the hydrogen permeation values in (3) to reach those achieved in (1) [24]. Wang and colleagues found that when they switched from nitrogen back to hydrogen it took less than a minute for hydrogen to permeate through the membrane [24]. These observations led Wang et al. to conclude that the increasing permeance trend under a hydrogen atmosphere was a result of the clearing of impurities from the active sites rather than a result of the unsteady state process [24].

In order to understand the full effect nitrogen has on hydrogen permeation, Wang et al. repeated their experiments on a fresh Pd composite membrane using

argon instead of nitrogen [24]. The membrane was heated in an argon atmosphere, subjected to hydrogen feed gas, exposed to argon, and then switched back to a hydrogen atmosphere again. The hydrogen permeation results can be seen in Figure 2-13 below. The hydrogen permeation data shown in Figure 2-13(a) reached a steady flux value after only roughly 200 minutes. The membrane was then subjected to an argon flow for several thousand minutes before the hydrogen flow was restored [24]. In Figure 2-13(b), it took only about 10 minutes for the hydrogen permeation values to reach those shown in Figure 2-13(a). When these results are compared with those shown in Figure 2-12, it is evident that nitrogen has a much greater effect on occupying the active sites than argon [24]. Now that similar experiments had been conducted using two separate pure inert gases, they decided next to explore the effect of using a hydrogen and nitrogen feed gas mixture.

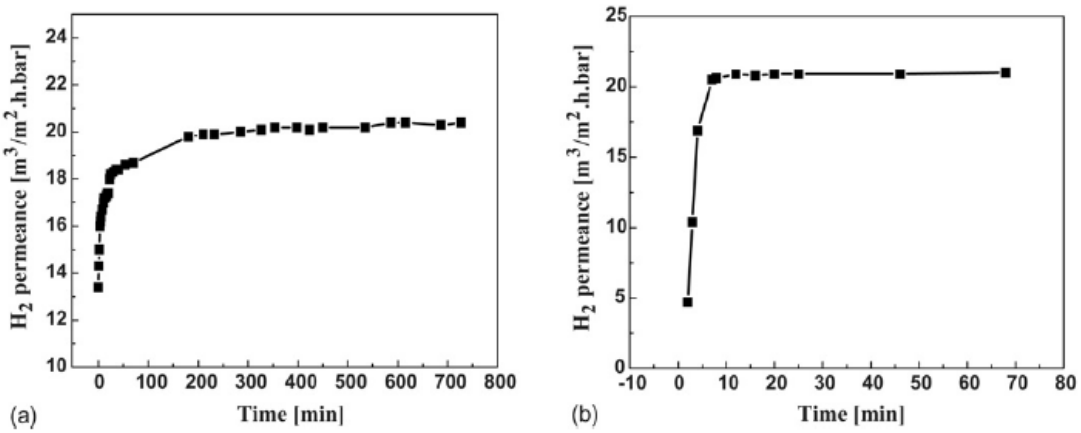

FIGURE 2-13. Hydrogen permeation results after (a) being heated in an argon atmosphere and (b) after being exposed to argon for several 1000 minutes at 550 degrees C [24].

Using a 1:1 molar H_2/N_2 ratio and a fresh membrane each time, Wang et al. measured the hydrogen permeance at various feed flow rates at 400 degrees Celsius

[24]. Each time it was found that the hydrogen flux remained steady for a period of time before gradually decreasing [24]. Wang and colleagues tested the membranes for leakage and determined that they were still intact after exposure to the H_2/N_2 flow [24]. Next they subjected the membranes to a pure hydrogen feed stream and found that the flux values decreased from the original mixture values. A further drop in permeation values was measured when the membranes were once again exposed to the H_2/N_2 mixture [24]. This led them to believe that the membranes had suffered from serious deactivation as a result of their inability to attain the original values after reactivation attempts using pure hydrogen [24]. Similar results were obtained when running the experiments at 450 degrees C. A trend was discovered at both temperatures that the higher the mixture flow rate, the more severe the drops in hydrogen flux through the membranes [24]. When the experiments were run once again at an even higher temperature of 500 degrees C, it was noticed that the H_2/N_2 mixture did not cause a drop in hydrogen permeance over a long time period. They therefore concluded that using thin Pd-ceramic composite membranes with a H_2/N_2 required operation at temperatures above 550 degrees C to prevent deactivation [24]. When operating below 550 degrees C, the membranes should be re-activated from time to time using a pure hydrogen feed gas [24].

Some studies have suggested the possibility of nitrogen reacting with hydrogen to form NH_x species. One study detected N_{1s} spectra by XPS on the surface of a Pd alloy after exposure to an 10% N_2/H_2 mixture gas, but it was unclear if any chemical species, such as NH_2, NH_3, NO or NO_2, were present on the surface [25]. Wang et al. believed the decrease in hydrogen permeance they experienced was a

result of the formation of NH_x (x=0-2) species on the surface of the membrane [24]. While there was no evidence that showed any permeation of these species through the membrane, they did act as an inhibitor to hydrogen permeation by occupying active sites [24]. Techniques have been presented to regenerate membranes believed to have been subjected to the formation of NH_x but will not be discussed here [24].

2.5.2 Water, Carbon Dioxide, and Carbon Monoxide

While much emphasis was placed on the negative effects of nitrogen in the previous section, there are several other gases that can be found in feed mixture gases that can lessen the hydrogen permeation rate. Carbon monoxide was found to have an even worse effect on hydrogen flux than nitrogen [26]. Gallucci et al. compared several studies of H_2/N_2 and H_2/CO mixtures and found that the negative effects of both CO and N_2 decreased with increasing temperature, but that carbon monoxide had an overall greater impact on hydrogen permeance than nitrogen [26]. Gallucci and colleagues further pointed out the theory that CO molecules could be interfering with the hydrogen flux through the Pd membrane by occupying active sites, increasing the hydrogen dissociation activation barrier, or a combination of both [26]. However, they were unable to develop a conclusion that supported the theory and instead only drew a partial conclusion.

Another study, conducted by Unemoto et al., displayed the effect of several hydrogen gas mixtures on the permeability values [3]. The experiments in this study showed that the following gases mixed in the feed had negative effects on hydrogen permeation values through a Pd-Ag membrane, from least to greatest: water vapor, carbon dioxide, and carbon monoxide [3]. However, a study by Guazzone, Engwall

and Ma found that steam only has a negative effect initially before gradually increasing hydrogen flux values to levels higher than those prior to steam application at temperatures in the 623-723 K range [27]. It is believed this is a result of H_2O molecules initially occupying active sites and blocking hydrogen. The flux starts to increase once the H_2O reacts with deposited carbon to form CO and H_2 [27]. After the steam application was ceased, the hydrogen flux increased even more before steadying, therefore reinforcing the idea that steam works to free the membrane surface of impurities [27]. However, there was an inhibiting effect due to the dehydrogenation of carbon monoxide and carbon dioxide that left carbon deposits on the surface of the membrane. Gradual carbon build up caused a decrease in the hydrogen flux through the membrane as a result of having CO and CO_2 in the feed [27].

2.5.3 Section Closing

The composition of the feed gas has a direct impact on the hydrogen permeation. The effect varies greatly and can sometimes be immediate or it can occur over time. Variables such as temperature, pressure and feed gas partial pressure values will also play a role in determining the outcome. Generally gases such as carbon monoxide, carbon dioxide and nitrogen have a negative effect. Argon has been shown to act inert and had a very limited effect while steam actually helped clear the membrane surface of impurities and increased the hydrogen flux. While many of the results in the literature showed similar effects across all membrane compositions, they sometimes varied from case to case. The make-up of the membrane is another important variable to consider in studying gas mixture

influences. Much of the focus in this section was on nitrogen due to its use in the experiments on which this thesis is based. It is important to note that some of these effects can be explained further by a more detailed study of the chemical kinetics at the membrane surface, but that will not be explored here.

Chapter 3: Experimental Setup

3.1 Membrane Characteristics

This project used palladium membranes mounted on porous stainless steel disks for all experiments. The membranes were prepared by Dr. Shamsuddin Ilias, a Research Professor in the Department of Mechanical and Chemical Engineering at North Carolina A&T State University (NC A&T), and the members of his research team. Four palladium based membranes were prepared at NC A&T for use in the Combustion Laboratory at the University of Maryland. The palladium was annealed after being mounted on the stainless steel supports and all characteristics were reported by the NC A&T research team. The palladium layer on Membranes I and II was reported to have a thickness of 10 microns while the layer on Membranes III and IV was 12 microns. The palladium covered the entire surface of one side of the stainless steel disk. The disks each had a one inch diameter, a thickness of 0.0625 inches and a 0.2 micron pore size. Figure 3-1 below shows Membranes I and II shortly after they were received.

FIGURE 3-1. Photograph of Membrane I (left) and Membrane II (right) before pressure testing.

Members of Dr. Ilias's team indicated that the palladium membranes should not be operated below 300 degrees Celsius as there is a risk of hydrogen embrittlement. This is concurrent with the findings in the literature regarding pure palladium membranes [1,5,12,13]. It was also suggested that the best operating temperature for these membranes is 350 degrees Celsius. It is important to note that the research team at NC A&T did not have experience running hydrogen separation experiments above 600 degrees Celsius or 30 psig.

3.2 Membrane Housing Design and Construction

The membrane characteristics were delivered prior to Membranes I and II and thus allowed for the design of the facility months before the first two membranes arrived. The first task was to design the membrane housing. From the literature, it was evident that the casing needed to be able to create a seal around the membrane

while also being able to withstand high temperatures and pressures. The casing would consist of two sides – the permeate side and the feed side. Each side was to have a gas inlet and outlet. The inlet on the feed side would be for the feed gas mixture while the outlet would be for feed gas output (gas that did not go through the membrane). The permeate side would have an inlet for the sweep gas and the outlet would be for the permeated hydrogen and sweep gas mixture.

The preliminary design consisted of three separate pieces that would be held together with machine screws. Initial drawings were completed by hand and in SolidWorks, the latter of which can be seen in Figure 3-2 and Figure 3-3 below. These components are shown in greater detail in the three view drawings in Appendix A. A key challenge to the design was determining how to make the casing easy to assemble and disassemble in order to have the ability to switch membranes while also maintaining a pressure seal during use. It was for this reason that the flange design was chosen in order to make it easy to seal with screws while also providing a way to tighten the casing uniformly.

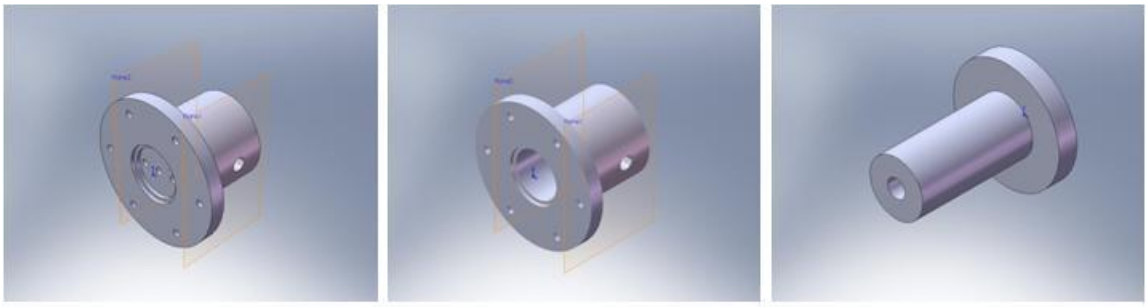

FIGURE 3-2. SolidWorks images of the three components that make up the Membrane Housing: the sweep side (a), the feed side (b) and the feed insert (c).

A gasket capable of handling high temperature and pressure was needed in order to provide the seal in the flange between the two pieces shown by Figure 3-2(a) and Figure 3-2(b). The gasket chosen for this task was a Novatec Premium II provided by All Custom Gasket. It is comprised of graphite and Kevlar and is capable of withstanding temperatures of 538 degrees Celsius (1000°F) and pressures up to 2500 psi [28]. Experiments were not planned to exceed 500 degrees Celsius or 100 psi making this gasket a good choice. The washers chosen to hold the membrane in place on both the feed side and permeate side were made of copper. The copper washers were sanded down using light machine oil in conjunction with both 600 and 1000 grit sand paper. This was done in order to remove the surface layer on the copper washers and eliminate any micro-sized grooves that could allow gas to escape.

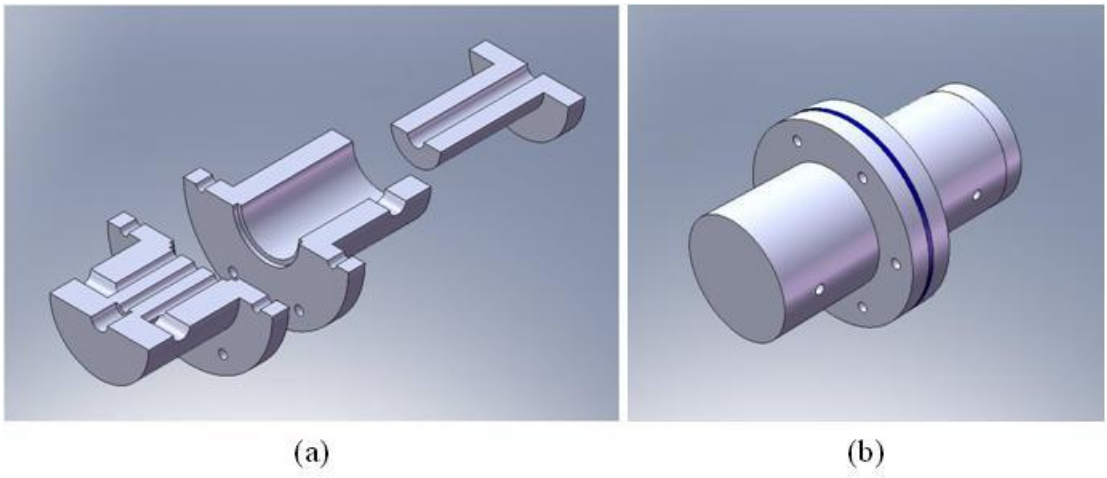

FIGURE 3-3. Horizontal cross-sectional view of Pd Membrane Housing design (a) and schematic of constructed Pd Membrane Housing (b).

One of the primary objectives when designing the feed side of the casing was maximizing the surface area to volume ratio. By decreasing the volume inside the feed chamber the amount of gas exposed to the membrane increases. If the feed chamber is too large, only a small percent of feed gas will actually come in contact

with the surface of the membrane, thus allowing a significant amount of hydrogen to exit the feed chamber without permeating. The copper washers chosen for use have a one inch OD and a 5/8 inch ID, therefore allowing a 0.3068 square inch surface area of the membrane to be available for hydrogen permeation. The feed inlet was designed with a 1/4 inch diameter and would direct the feed gas directly at the center of the membrane, flowing outward and around the feed insert piece to the feed outlet, as shown in Figure 3-4 below.

The feed inlet piece was designed with a length that would allow it to be just a 1/16 inch away from the copper washer sealing the feed side of the membrane. This 1/16 inch gap plus the 1/16 inch thick copper washer meant that the mouth of the feed inlet would be 1/8 inches away from the membrane surface. Extruding the exposed membrane surface area out against the mouth of the feed inlet yielded a membrane-feed exposure volume of 0.0384 cubic inches and a surface area to volume ratio of eight. Making this ratio any smaller would cause less feed gas to pass directly over the surface of the membrane. On the contrary, making it larger would allow more feed gas to be exposed to the membrane, but could lead to flow constriction and pressure build-up inside the casing (assuming the ratio would be made larger by making the feed insert longer).

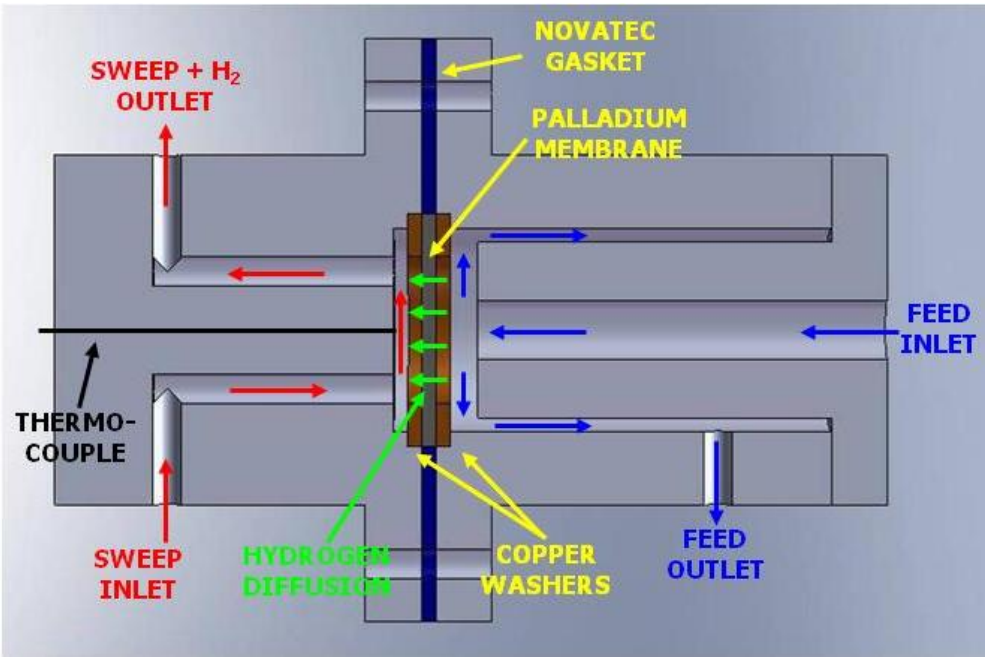

FIGURE 3-4. Schematic cross-section of Pd Membrane Housing.

It was determined due to the high temperatures and pressures to which the housing would be exposed that stainless steel should be used as the casing material. Type 303 stainless was selected due to its machinability. The feed and sweep components were made from a rod with a 2-1/2" diameter while the feed insert was made from a 1-1/2" diameter rod, both of type 303 stainless steel. Once machining on the components was complete, the feed insert was welded to the feed side and Swagelok® fittings were welded in place for the gas inlets and outlets as well as the inlet for the thermocouple. It was suggested that the Swagelok® fittings would be less likely to leak if they were welded in place in the holes rather than tapped. The completed feed side and sweep side components can be seen in Figure 3-5 and Figure 3-6 below, respectively. A more detailed depiction of the individual components on the feed and sweep sides can be seen in Figure 3-7 and Figure 3-8 below, respectively.

FIGURE 3-5. Membrane housing feed side.

FIGURE 3-6. Membrane housing sweep side.

The six holes drilled in the outer edge in Figure 3-5 and Figure 3-6 are 0.1285 inch diameter clearance holes for the 5-40 machine screws used to hold the casing together. Five Swagelok® fittings were welded in place on both casing pieces. All five fittings are connecters for 1/4" male NPT to 1/8" tube OD. Four of the fittings are 90 degree elbows and the fifth one is a straight. The purpose of each fitting and the other features on the casing is labeled in Figure 3-7 and Figure 3-8 below. The copper washers and Novatec gasket can be seem with Pd Membrane III in Figure 3-9.

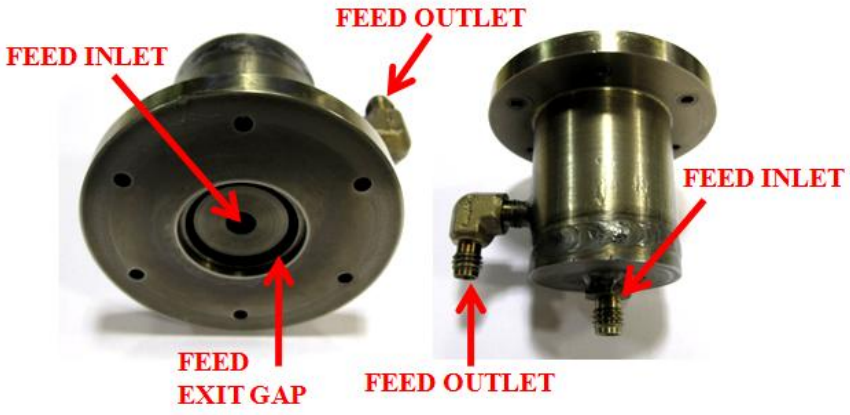

FIGURE 3-7. Membrane housing feed side components.

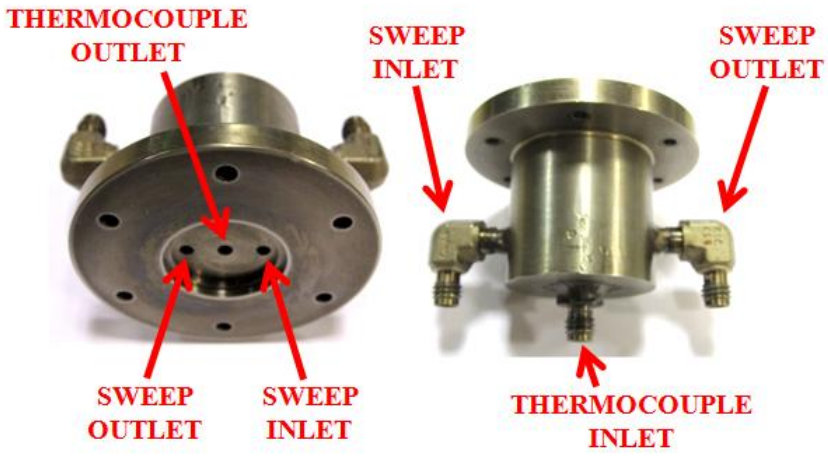

FIGURE 3-8. Membrane housing sweep side components.

FIGURE 3-9. The copper washers, Novatec gasket and Pd Membrane III.

The two copper washers are used to hold the membrane in place inside the casing, while the gasket provides the seal between the feed and sweep surfaces. Putting the casing together is a task that requires a degree of precision to ensure that each of the six machine screws are tightened uniformly. Otherwise there is the risk that leaks may form as a result of a loose screw or a screw that's been over tightened on one side. The order in which the screws were tightened can be seen in Appendix B. The screws were tightened using a torque screwdriver so that the same amount of torque was applied to each screw during the tightening process. The screws were tightened using up to 20 in-lb of torque. Figure 3-10 below shows the casing completely assembled with washers, membrane, and Novatec gasket in place. The casing as displayed is ready for use in the hydrogen separation facility.

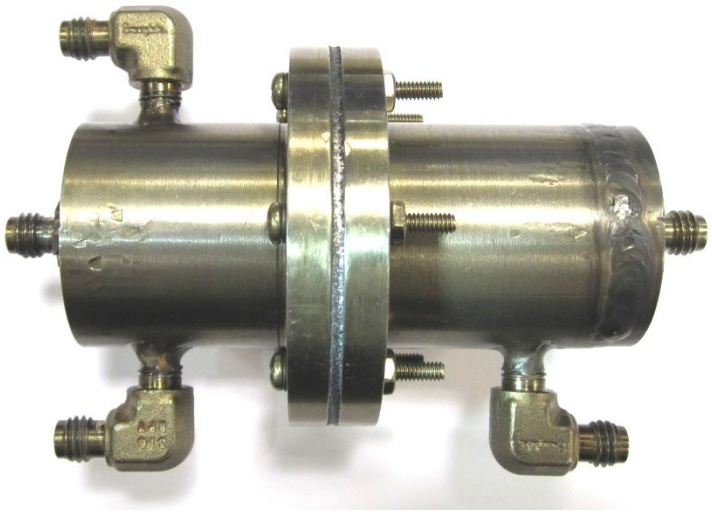

FIGURE 3-10. Membrane casing assembled with washers, membrane and Novatec gasket in place.

3.3 Hydrogen Separation Facility Design

The hydrogen separation setup used for these experiments mirrors in a lot of ways what is found in the literature. It contains the basic control mechanisms and devices to incorporate both a feed mixture and a sweep gas. The system was designed to have a two mixture feed gas, but additional gases could be added after making minor modifications to the facility. The sweep gas was designed with a cross-connect valve such that it could be used on the feed side, the sweep side, or both. It is used on both sides during heating and cooling operations and on the sweep side during hydrogen separation experiments. The feed stream exiting the feed side of the membrane casing goes directly to vent. However, the system could be modified such that the feed outlet gas is recirculated and passed over the membrane additional times. The gas mixture leaving the permeate side of the membrane

housing is directed towards a Gas Chromatograph for analysis. A schematic diagram of the facility can be seen in Figure 3-11 below.

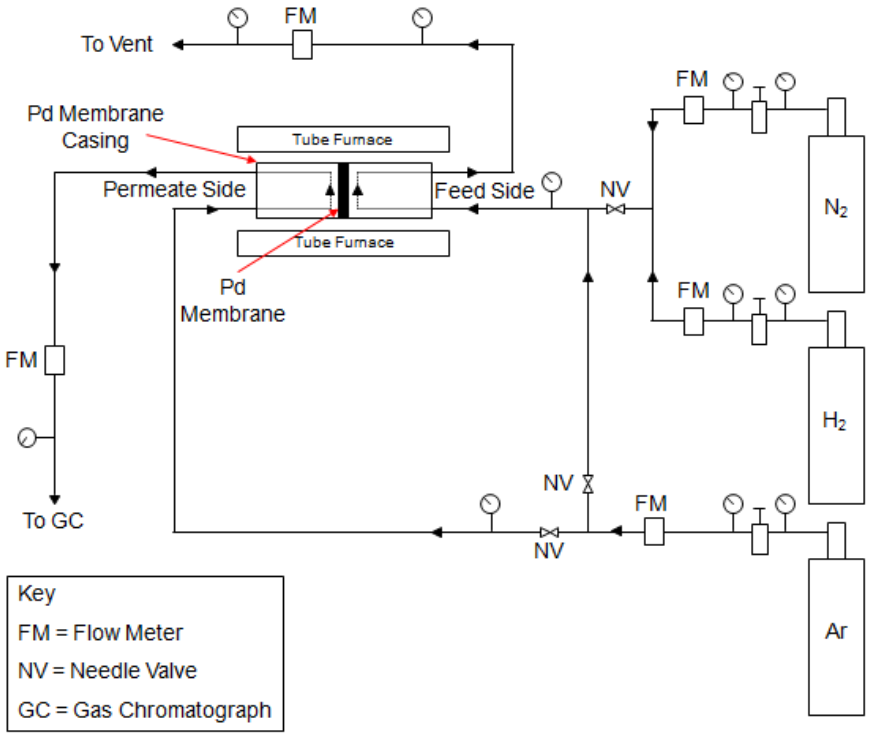

FIGURE 3-11. Line drawing of Hydrogen Separation Facility and components.

The system has five flowmeters in place in order to monitor as well as regulate gas flow. Each flowmeter has a valve in place at the base that is used to make flow adjustments. The flowmeters are placed in key positions throughout the setup. Each gas line has a flow meter after the gas bottle regulator. A flowmeter was put in place after the permeate side outlet in order to maintain the proper pressure differential on the membrane. One was also placed immediately after the feed side outlet for the same reason. Pressure gauges are placed throughout the system in order to monitor the pressure. The flowmeter and pressure gauge locations can be viewed in Figure 3-11.

Initial pressure tests on the facility and Membranes I and II were conducted prior to facility completion. The initial experiments were conducted without the inclusion of the second feed gas and without flowmeters in place. These were added later for the pressure testing on Membrane III and the experiments conducted with Membrane IV. A view of the completed facility can be seen in Figure 3-12 below. The furnace in use is a Carbolite Model HST 12/--/300/301 Single Zone Hinged Tube Furnace. It has a heated length of 11.75 inches and can accommodate a tube OD of 4 inches. The maximum temperature to which the furnace can heat is 1200 degrees Celsius. The GC used for these experiments (not pictured) is an Agilent 3000 Micro Gas Chromatograph.

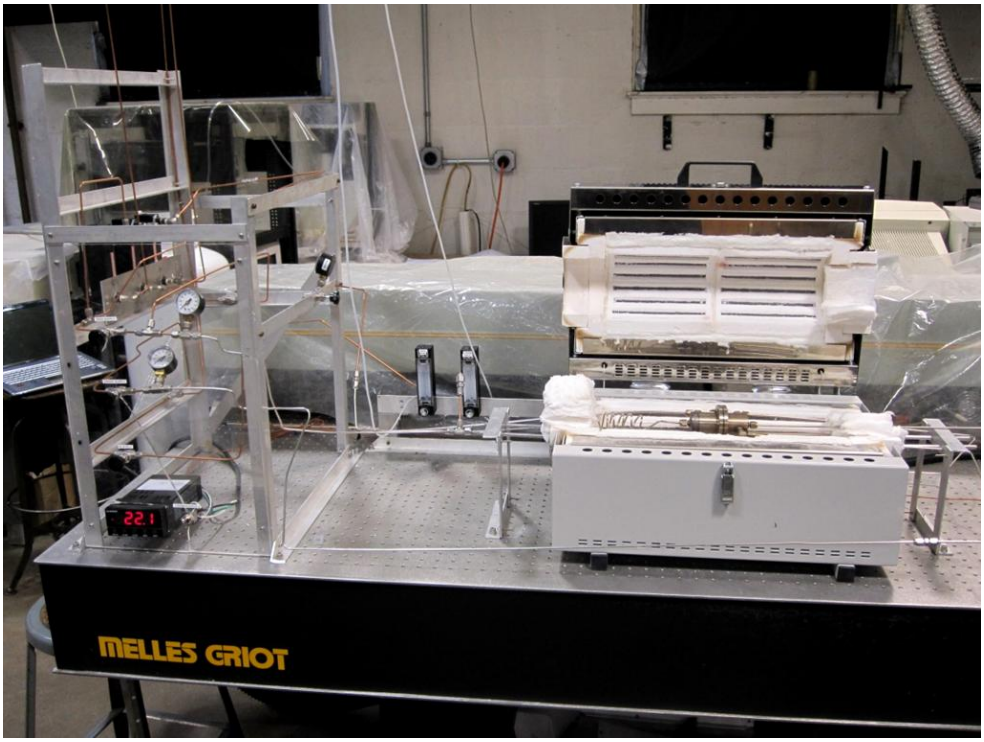

FIGURE 3-12. Hydrogen Separation Facility in the Combustion Laboratory at the University of Maryland.

When placed inside the tubular furnace, the membrane housing rests on two 1/8” steel rods. The gas lines are attached to the Swagelok® fittings as shown in Figure 3-13 below. The thermocouple is inserted into the Swagelok® fitting on the sweep side of the housing and secured to prevent leakage.

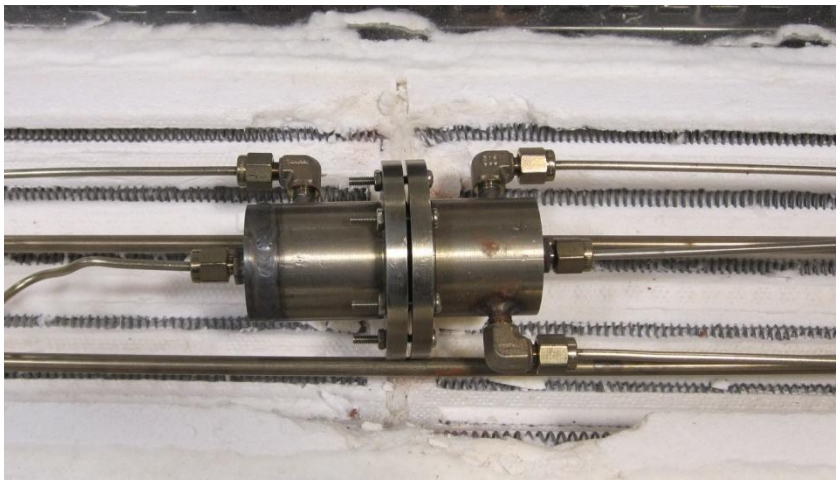

FIGURE 3-13. Membrane housing mounted inside tubular furnace.

The description of the hydrogen separation facility, as stated above, is the current configuration of the system. Several pressure tests were conducted during facility construction – both on the facility itself and on Membranes I and II. Experiments were conducted once the flowmeters and second feed gas were integrated into the setup. While this current system was adequate for completing the desired experiments, it was designed in such a way that modifications could be easily made for further research. Recommendations for future modifications will be discussed in Chapter 6.

Chapter 4: Uncertainty Analysis

4.1 Measurement Chain

The measurement chain provides a way to differentiate between actual and measured values. It consists of the measured value, error associated with the measurement, correction terms for the error and linked uncertainties, and the uncertainty related to the measurement. The general equation for a measurement chain can be seen below in Eqn. (4-1).

$$M_{corr} = M_{undist} - \sum E + \sum C \pm \delta C \pm \delta M_{obs} \quad (4\text{-}1)$$

The error and correction terms were neglected and the uncertainty analysis was primarily focused on the δM_{obs} value. Therefore, Eqn. (4-1) can be simplified to Eqn. (4-2).

$$M_{corr} = M_{undist} \pm \delta M_{obs} \quad (4\text{-}2)$$

The overall uncertainty of the measurement can be found by applying Eqn. (4-3), the root sum square (RSS) method.

$$e_r = \sqrt{\sum \left(\frac{\partial f}{\partial x_n} e_n\right)^2} \quad (4\text{-}3)$$

Using RSS will allow for the derivation of the expression to be used for the δM_{obs} term in Eqn. (4-2).

4.2 Sources of Uncertainty

Anything that takes a measurement will always have some uncertainty associated with the measured value. Sometimes certain sources of error or bias can be neglected while other times they must be considered in achieving a corrected value. In the case of the experiments conducted in this study, the sources of error were primarily the pressure gauges, the thermocouple, the flowmeters and the GC. These sources could vary in relevance depending on the scope of the experiment and measurements taken. The uncertainty analysis was conducted on measurements for the flow, pressure, temperature and the GC.

The values for the uncertainty of the pressure and temperature measurements were not found using the RSS method. Since there were no elaborate equations or computer software used to determine these measurements, the uncertainty in the measurements was assumed to be the given error for the specific instrument. In the case of the pressure gauges, the reported accuracy was ±2% mid-scale [29]. As for the thermocouple, the error was reported to be ±2.2°C or ±0.75%, whichever is greater [30]. Due to the temperature ranges used in the experiments, the latter error was used for the thermocouple readings. The accuracy reported for the rotameters was ±3% [30].

The manual for the GC did not report any error or accuracy values for gas samples and thus required a different approach. Three GC measurements were taken at each sample location during all experiments. The standard deviation for the three values was then used to find a 95% confidence interval. The confidence interval was then assumed to be the error associated with the GC for each measurement. The

percentage of hydrogen leaked was found using the GC concentration percentages for the gases. The leak equation uses the gas percentage values from the feed and permeate sides to determine the percentage of hydrogen that leaked through the membrane rather than permeated. This relation can be viewed in Eqn. (4-4) below.

$$H_L = \frac{[N_2]_p[H_2]_f}{[N_2]_f[H_2]_p} \tag{4-4}$$

Applying Egn. (4-3) to Eqn. (4-4) yields the following relation for the uncertainty associated with the leak percentage value.

$$\delta M_{obs} = \left[\left(\frac{[N_2]_p}{[N_2]_f[H_2]_p}e_{H_{2,f}}\right)^2 + \left(\frac{[H_2]_f}{[N_2]_f[H_2]_p}e_{N_{2,p}}\right)^2 + \left(-\frac{[N_2]_p[H_2]_f}{{[N_2]_f}^2[H_2]_p}e_{N_{2,f}}\right)^2 + \left(-\frac{[N_2]_p[H_2]_f}{[N_2]_f{[H_2]_p}^2}e_{H_{2,p}}\right)^2\right]^{1/2} \tag{4-5}$$

The e_n values in Eqn. (4-5) are the values of the 95% confidence interval associated with each measurement. However, since the δM_{obs} values varied between experiments, the largest value was chosen and applied to all of the measured values. In other words, a conservative approach was used where the largest uncertainty value was used to correct each measured value. The same approach was used to find the uncertainty in the calculations for the actual flow rates, the gas flux values, the selectivity, the pressure exponent and the activation energy. Often times, the uncertainty had to be further broken down to find the uncertainty within a single uncertainty term. Displaying the details of the uncertainty analysis for each calculation is tedious and is not shown here, but the uncertainty is shown in the form of error bars on the plots in Chapter 5.

Chapter 5: Experimental Results and Analysis

5.1 Pressure Testing – Facility

As was stated in Chapter 3, initial pressure testing on Membranes I and II was conducted prior to completion of facility construction. All major components were in place with the exception of the second mixture gas and the flowmeters. Prior to subjecting the membranes to testing, the setup was put through several trial runs using argon gas to ensure there was no leakage from any of the fittings.

It was during the trial runs that it was discovered the facility could not hold pressure and subsequently experienced a pressure drop. The first 5 tests were conducted without the membrane or copper washers in place, but the Novatec gasket was used to create a seal between the surfaces of the two casing pieces. The results of the five tests can viewed in Figure 5-1 below. Using a soap and water solution, the leaks were found to be coming from between the gasket and the faces of the membrane casing. After the first three tests failed, the flat surfaces of the membrane casing were sanded to create a smoother surface. The sanding was done using a light application of machine oil and 600 grit sandpaper. After some time, the 600 grit sandpaper was replaced by 1000 grit sandpaper. Once the surfaces were smooth they were cleaned to remove any particles or oil residue left over from the sanding process.

It is evident by the trend shown for Test 4 in Figure 5-1 that the sanding had very little effect as the leak was still present. Considering the experiments were to be conducted above 300 degrees Celsius, it was felt that perhaps attempting the pressure test at a higher temperature would be more successful as thermal expansion of the casing may create a better seal. This assumption proved to be correct as the results of Test 5 in Figure 5-1 show a much slower leak rate.

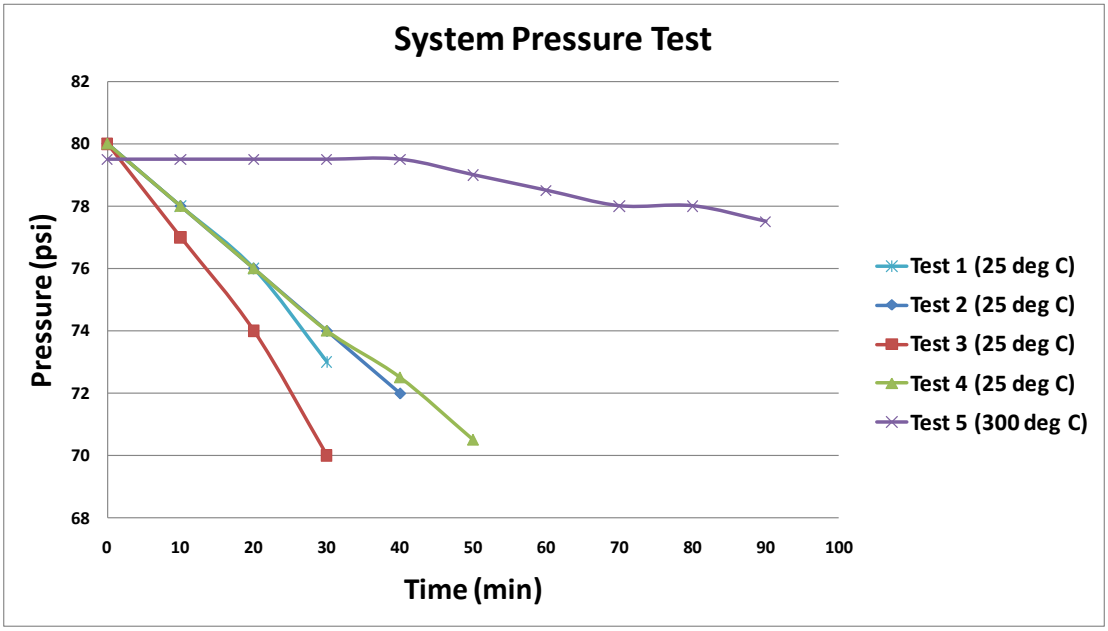

FIGURE 5-1. Hydrogen separation facility pressure testing results. Tests 1-4 were conducted at room temperature while Test 5 was conducted at 300 degrees Celsius.

Even with improved results there were still two problems: 1) the casing was still leaking, and 2) the casing still needed to be tested with the membrane and copper washers in place. Therefore the next test was with the membrane and washers inside the housing. The casing was once again heated to 300 degrees Celsius and argon gas applied at a pressure of 80 psig. Argon was applied simultaneously to the feed and permeate sides via the sweep gas cross-connect valve as to not cause a pressure

difference between the two sides of the membrane. The pressure drop was by far more significant than any drop seen in the first five tests as is shown in Figure 5-2 below.

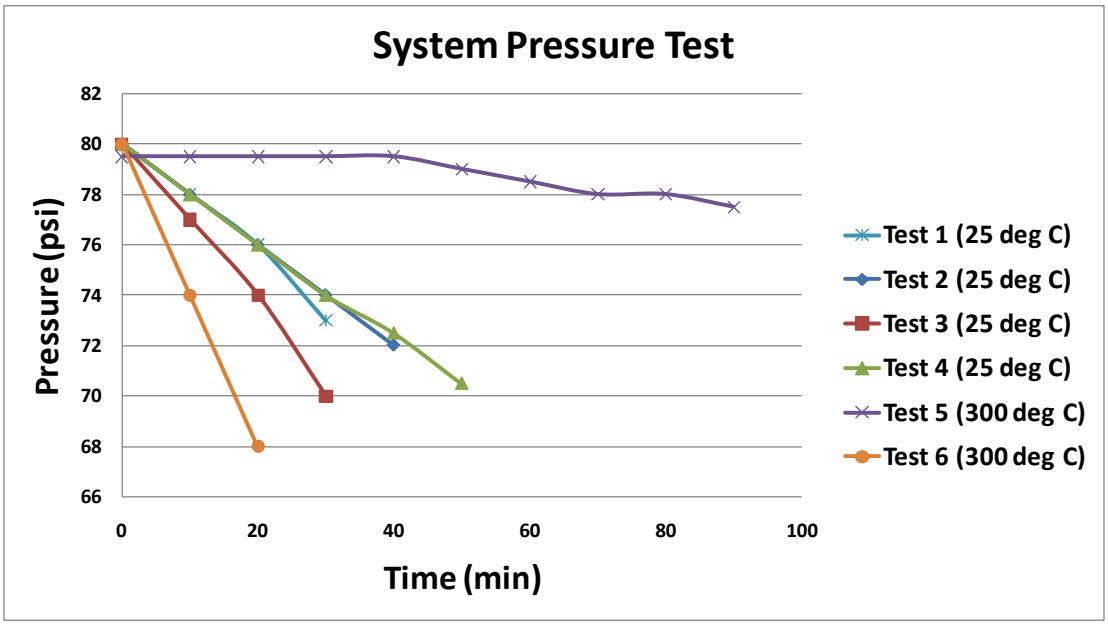

FIGURE 5-2. Hydrogen separation facility pressure testing results. Test 6 was conducted with all components in place inside the membrane housing.

The results of the first six tests made it rather evident that the problem was creating a seal between the two faces of the sweep and feed sides of the membrane housing. The best results came at a temperature of 300 deg C without the membrane and washers in place. Once the membrane and washers were secured inside casing, the worst leak rate of the six tests was recorded. It was clear at this point that the addition of the membrane and washers interfered with tightening the six screws enough to create a good seal on the gasket. With this in mind, the next course of action was to test the casing without the Novatec gasket in place.

In order to test the casing without the gasket in place a third copper washer had to be secured in place of the membrane. The reasoning for this was due to the

fact that the membranes only have a Pd layer on one side of porous stainless steel disks. The edges of the membranes are not coated with Pd and therefore gas can leak radially through the porous support. The third washer, like the other two already in place, had been sanded as previously stated prior to testing. The screws were tightened with the washers in place and the casing was inserted into the system. A computer image of the modified casing setup can be viewed in Figure 5-3. Test 7 (without the Novatec gasket) was conducted at room temperature and a pressure of 78.5 psig. This test was carried out over a 16 hour period and no pressure drop was recorded during this time. The next trial run, Test 8, was then conducted at 317 degrees Celsius for 3 hours and it too did not experience any gas leakage.

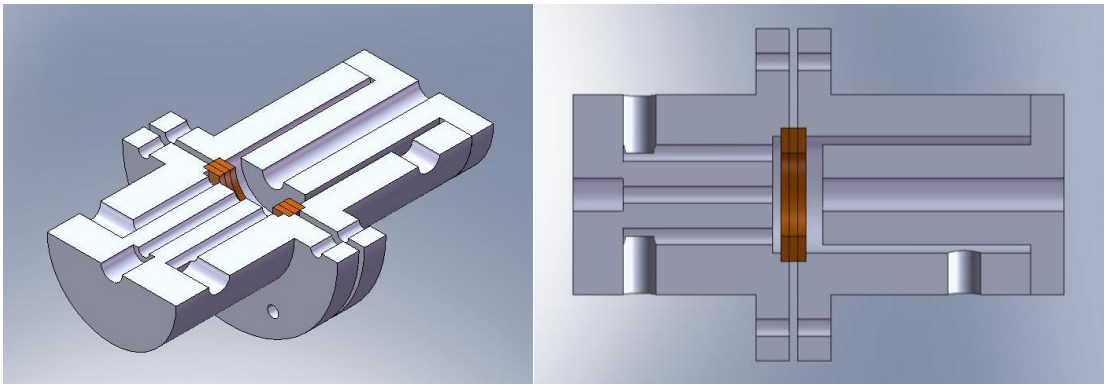

FIGURE 5-3. SolidWorks cross-sectional view of the modified casing without the gasket and a third copper washer in place of the Pd membrane.

The three copper washers compressed together created a seal that prevented a pressure loss inside the facility at both room temperature and elevated temperature. It was concluded that the Novatec gasket was the primary reason for the pressure loss in the previous tests. Ascertaining the source of the leak meant trials could now be carried out using the membranes. The purpose of these tests was to determine whether or not the Pd layer on the membranes was intact. Initial visual inspection of

Membranes I and II at 30x magnification revealed some very small scratches. There were also dark spots present on the surface of the membrane that could perhaps be areas of incomplete coverage. The scratches were cause for concern about the integrity of the Pd layers on the porous support.

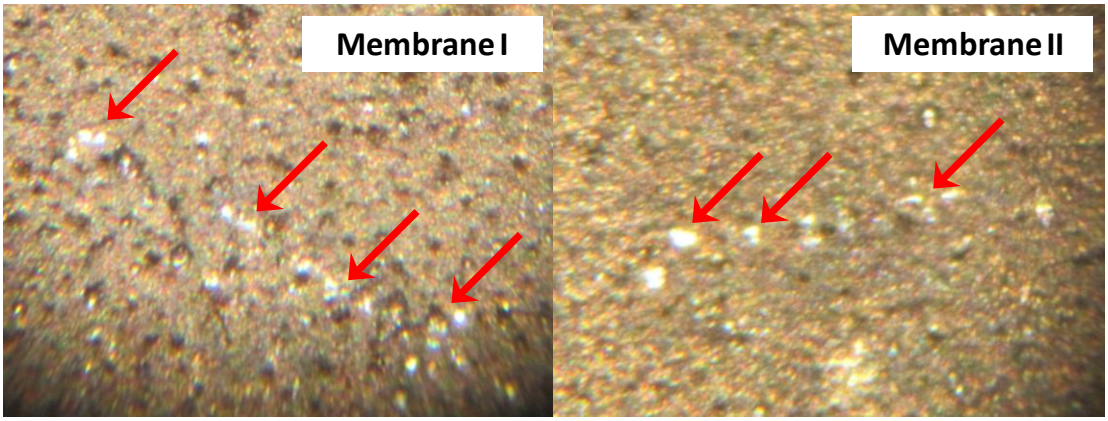

FIGURE 5-4. Images of the Pd surface on Membranes I and II. Areas of incomplete coverage are indicated by the red arrows. The dark spots are also suspect, but are not as apparent as the areas where the stainless steel below the Pd layer is visible.

5.2 Pressure Testing - Membranes

5.2.1 Testing Membranes I and II

Membranes I and II were both subjected to the same pressure test. They were sealed separately inside the membrane housing with the Pd layer facing towards the feed side. Since the purpose of this experiment was to determine whether or not the membrane would leak, there was no need to apply any more than 10-15 psig of argon on the feed side. This was not viewed as a concern as the members of Dr. Ilias's research team at NC A&T had said they had experience with the membranes up to 30 psig, as stated in Section 3.1. In the absence of the gasket, the sides of the membrane were exposed. With no Pd coating on the edges of the membrane any gas diffusing

through the membrane would leak radially. This was not foreseen to be a problem as the assumption was that the Pd layer was intact and the test gas (argon) would not be able to pass through. However, this was not the case and both membranes experienced leaks.

Since the feed gas consisted of argon only, there should have been no pressure drop once the gas was applied to the feed side. This meant that the feed side pressure gauges should have remained at a constant value while the pressure gauges on the permeate side should have remained at zero. In reality, the pressure dropped on the feed side and rose on the permeate side. This was a sign that gas was passing through the membrane and pressurizing the permeate side of the facility. Since there was no seal on the edge of the membrane, any pressure loss around the membrane would have been to the environment. The fact that the pressure increased on the permeate side indicates argon had to have been going through the membrane. The only way for this to be possible was if the Pd layer on the membrane was not intact. This confirms the original suspicion that the scratches on the Pd side of the membrane had compromised the integrity of the Pd layer.

5.2.2 Testing Membranes III and IV

The pressure tests on Membranes III and IV were conducted using the same process as was used to test Membranes I and II. The only exception was that the applied feed pressure was much lower and did not exceed 2.0 psig. In both cases the pressure increased on the permeate side as soon as the gas was applied on the feed side. Once again this showed that the Pd layer on both membranes had been compromised prior to testing. The membranes were further examined under a

microscope at 30x magnification which can be viewed below in Figure 5-5. While both membranes exhibited defects, Membrane III clearly had more notable flaws than Membrane IV. In several places it appeared that the Pd layer was flaking off the stainless steel support of Membrane III. On the other hand, Membrane IV mostly displayed small areas of incomplete coverage or minor scratches.

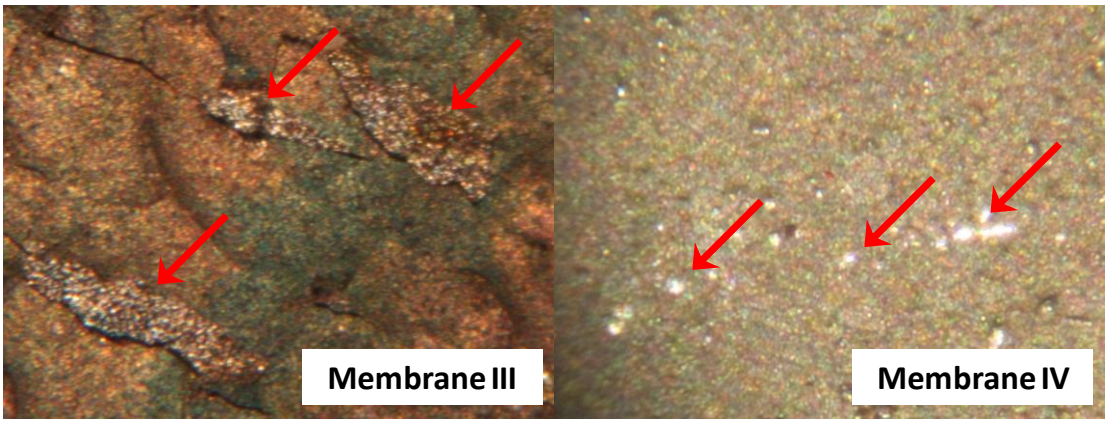

FIGURE 5-5. Images of the Pd surface on Membranes III and IV. Areas of incomplete coverage are indicated by the red arrows. The Pd layer on Membrane III seems to be flaking off the surface of the stainless steel support.

The results of the tests on Membranes III and IV were concurrent with what was seen during the tests of Membranes I and II. The reasons for the defects on the membranes are unknown and were not explored. It can be assumed that the faults in the Pd layer are the result of the membrane preparation process or damages due to the shipping process. Regardless of the cause, the pressure tests on all four membranes revealed that the Pd layers failed to establish a diffusion barrier. This unforeseen circumstance presented a new challenge in studying the permeation of hydrogen in the experiments to come.

5.2.3 Membrane Shear Stress Calculation

In order to rule out the possibility that the membrane failed due to the pressure of the feed gas certain calculations had to be considered. Eqn. (2-9) could be used to determine the maximum allowable pressure for a thin ductile membrane. While the Pd layers on these membranes are roughly 10 microns and can be considered thin and ductile, the membranes are supported. Eqn. (2-9) does not take into account the addition of a porous support. Since there are areas of the membrane that can be considered unsupported due to the presence of pores in the stainless steel media, it is possible to use these areas for the calculation of Eqn. (2-9). The pore size of the stainless steel support is 0.2 microns. The thickness-pore size ratio is 10:0.2, or 50:1. Therefore, the membranes in this experiment can't be considered "thin" when compared to the miniscule pore size. This dismissed the use of Eqn. (2-9) for these calculations.

The method used instead of Eqn. (2-9) involved a shear stress calculation and yield strength comparison. Assuming a feed pressure of 1000 psi is used, which is much higher than any pressure used experimentally in this setup, the following calculations have been completed to determine if the palladium could withstand the pressure in unsupported areas (i.e. where there are pores in the stainless steel). With a diameter of 0.2 microns, the cross-sectional area of the pore is as follows:

$$A_p = \pi \left(\frac{d_p}{2}\right)^2 \tag{5-1}$$

Eqn. (5-1) yields a pore cross-sectional area of 4.869E-11 in^2. Knowing the pressure and the cross-sectional area, the force acting on the palladium over the unsupported area can be calculated.

$$P = \frac{F}{A} \Rightarrow F = P * A_p \quad (5\text{-}2)$$

Using Eqn. (5-2), the force acting on the palladium unsupported by a stainless steel pore was found to be 4.869E-8 lb. To determine the amount of shear that results from this force, the force had to be divided by the shear area. The shear area is the thickness of the membrane multiplied by the perimeter length of the pore as denoted by A_s in Eqn. (5-3) below.

$$\tau = \frac{F}{A_s} \quad (5\text{-}3)$$

The shear stress acting on the palladium unsupported by the pore is 5.00 psi. The yield strength is temperature dependent and generally decreases as temperature increases [19]. The reported range for the yield strength of Pd is between 35 and 205 MPa, or 5,076 and 29,733 psi [19,31]. It is therefore evident that even at pressures up to 1,000 psi, there will be no deformation as a result of the unsupported palladium at stainless steel pore locations. Assuming the reported pore size of 0.2 microns is an average, there is the possibility of larger pores and this must be considered. For example, if a feed pressure of 1,000 psi was applied and there was a pore with a 100 micron diameter present, the shear stress would be 2,500 psi. Simply put if there was a pore in the stainless steel material that was 500% of the reported pore size, the shear stress would still be lower than the yield strength.

5.3 Permeation Experiments

The fact that all four membranes had defective Pd layers meant that the gas leakage aspect would have to be examined as well. After completing the pressure testing on the membranes with unfavorable results, a membrane was selected from

the group to undergo further testing. Each membrane was examined via microscope at 30x magnification and the membrane with the least apparent surface defects was chosen. Looking at Figure 5-6 below, in which all four membrane surfaces are shown, it is reasonable to assume that Membrane IV appears to be in the best condition. As such, Membrane IV was used from this point forward for all experimental trials.

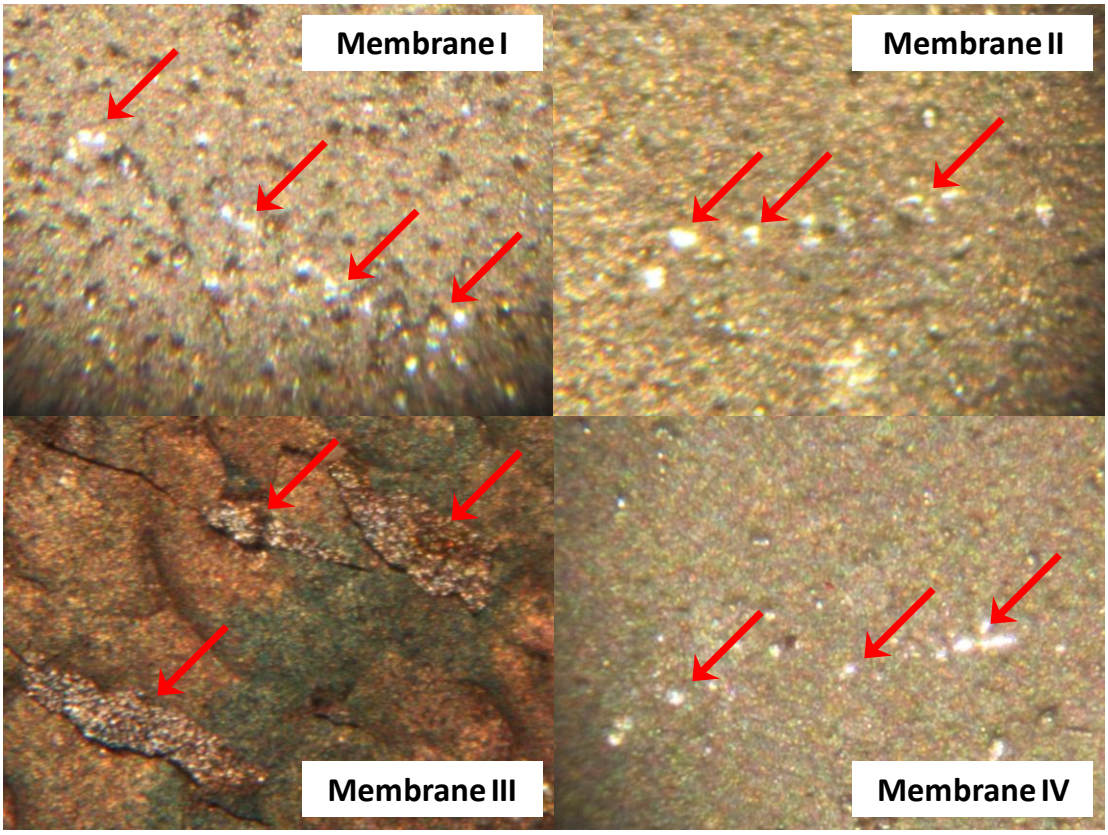

FIGURE 5-6. Comparison of the surface images of Membranes I-IV at 30X magnification. Membrane IV appears to have the least surface defects.

5.3.1 Checking for Hydrogen Permeation

Knowing ahead of time that the feed gas would leak through the defects in the Pd surface layer required a modification to the approach. The first objective was to ensure that hydrogen would actually permeate through the membrane. The next

objective was to study the effects of varying the temperature and total pressure of the system on the permeation to leak ratio. This second objective will be discussed extensively in the next section.

Permatex® High Temp Red RTV Silicone Gasket Maker was applied around the edge of the membrane in an attempt to prevent radial leakage. This was done just prior to casing assembly. The membrane was sealed in place inside the casing between two copper washers without the Novatec gasket. The housing was allowed to sit for a 24 hour period in order for the gasket maker to fully cure. It was later found that the gasket maker didn't work and gas leaked radially from the membrane. While it was preferred that the casing wouldn't have any leaks, this was accepted due to the fact that it would have a minimal effect, if any, on the experiments to come. The following day, the casing was placed inside the tube furnace and the Swagelok® fittings were secured.

Gas samples were taken at three locations in the facility to test the membrane for permeation. The locations can be viewed in Figure 5-7 below. The first location (1) is just before the feed gas mixture enters the casing. The second location (2) is after the feed gas leaves the casing while the third (3) is on the permeate gas line leading from the membrane housing. It was important that the gas was tested at these three sites specifically. Sampling at location (1) gives the feed gas composition prior to entering the membrane housing, location (2) gives the feed gas composition after it is exposed to the surface of the membrane and location (3) yields the permeated gas results. Three samples were taken at each location in sequential order at 325 degrees Celsius. The feed gas mixture consisted of hydrogen and nitrogen and was held

constant using the flowmeters. The pressure upstream of the membrane was maintained at 15 psig. The sweep pressure was 0 psig for sampling at locations (1) and (2), but was held at 3.0 psig for sampling at location (3). The reason for this is that an argon sweep gas had to be used in order to get enough flow at location (3) for the GC to sample the gas mixture.

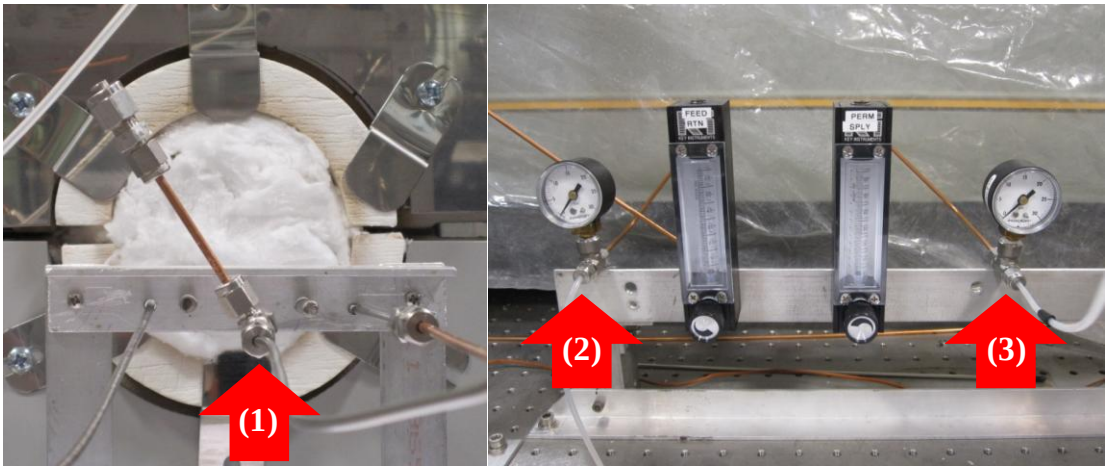

FIGURE 5-7. The three gas sample locations for GC analysis: (1) feed inlet, (2) feed outlet and (3) permeate.

The results for the permeation test are shown in Figure 5-8 below. The GC detected H_2, N_2, O_2 and CO_2 in each gas sample, but the O_2 and CO_2 amounts were negligible compared to H_2 and N_2 and are not shown in Figure 5-8. The three samples at each location were averaged for each gas to produce the results shown in the below figure. The values are expressed in % composition per mole of gas. The feed gas consisted of 36.9% H_2 and 58.0% N_2 (out of 95.9% sampled) at location (1). These values were used as a base for comparison for the other two sample locations. At location (2), the gas mixture was 36.0% H_2 and 59.4% N_2 (out of 96.3% sampled). The hydrogen concentration was slightly lower than that at location (1) and the nitrogen concentration was slightly higher. This shows that even with the faulty

membrane, more hydrogen was going through than nitrogen. This was further solidified by the results at location (3).

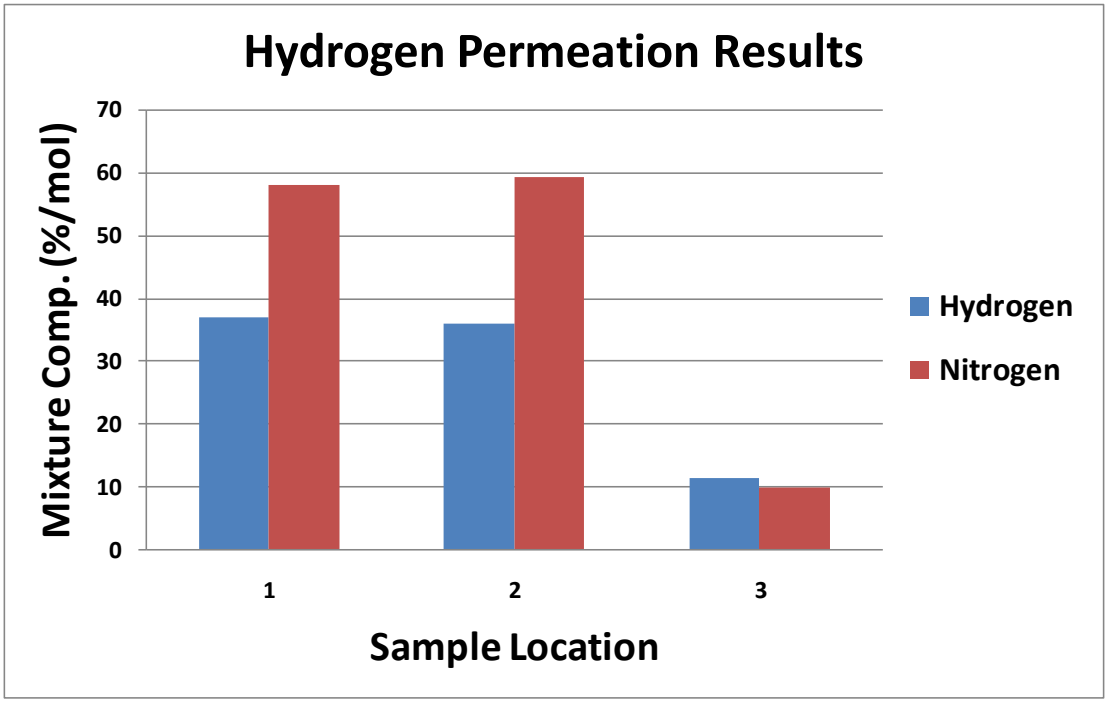

FIGURE 5-8. Permeation test results. Comparison between (1) and (3) shows that while Nitrogen is leaking through the membrane, hydrogen is permeating.

The gas composition at location (3) was much different from that at the other two locations due to the addition of argon as a sweep gas. The Agilent 3000 Micro GC lacks the ability measure argon. It will account for the fact that another gas is present, but it will not identify it. In this case, the remainder of the gas not detected can be assumed to be argon. The results for location (3) yielded 11.4% H_2 and 9.8% N_2 (out of 22.3% sampled). This differs from locations (1) and (2) in that the concentration of hydrogen is greater than that of nitrogen. This confirms suspicion after testing at location (2) that while nitrogen is passing through the membrane, the hydrogen concentration is greater on the permeate side due to the added effect of

hydrogen permeation. The presence of the nitrogen on the permeate side could lead some to question whether or not nitrogen is in fact permeating through the membrane along with the hydrogen. However, this is very unlikely and will be discussed later. The greater hydrogen than nitrogen concentration on the permeate side confirms that the membrane is still functioning despite the surface faults and allows for the next objective to be addressed. Using what was leaned during the permeation test, certain assumptions were made in order to determine the percentage of hydrogen permeated versus leaked. Knowing this enabled further examination of temperature and pressure effects on the hydrogen permeation to leak ratio.

5.3.2 Effects of Membrane Defects on Permeation

The primary assumption moving forward with these experiments was that the gas leaking through the membrane maintained the same ratio as was present in the feed. That is, the gas concentrations of the mixture that leaked through the faults in the membrane's Pd layer were assumed to be the same as the gas composition at sample location (1). By using this information and knowing the concentration of hydrogen and nitrogen on the permeate side, the leak ratio was applied in order to determine the amount of hydrogen that was permeated versus leaked. Analyzing the effects of varying temperature and pressure of the system on hydrogen permeation will be the primary goal in this section.

Five different experiments were conducted in order to complete this analysis, with one of the experiments (350°C, 15 psig) being used as a data point twice. Three of the experiments were carried out at constant pressure (15 psig) and varying temperature (325°C, 350°C, 375°C), while the other three were done with constant

temperature (350°C) and the changing pressure (10 psig, 15 psig, 20 psig). The feed gas was maintained at a constant level using the flowmeters as was done in the first experiment. The sweep pressure was maintained at 3 psig, while the permeate pressure at location (3) was atmospheric. The system conditions were adjusted (if needed) between each sample to ensure consistent operating parameters. The feed gas composition was made up of nitrogen and hydrogen, while argon was used as a sweep gas only when sampling at location (3).

Each experiment was carried out using the same procedure; the only differences between experiments were variances in temperature and feed pressure. The membrane casing was heated using a step rate of 25 degrees Celsius per minute under an argon atmosphere. Hydrogen gas was only applied at temperatures above 300 degrees Celsius. At the completion of each experiment the membrane was exposed to pure hydrogen for 30 minutes in an attempt to clear the surface of any impurities as was suggested by the literature [24]. After hydrogen regeneration, the hydrogen gas was then cleared out of the system by argon and the membrane was cooled in an argon atmosphere.

The results from the experiments where temperature was constant are shown in Figure 5-9 while the results for constant pressure are shown in Figure 5-10. During the experiments hydrogen traversed through the membrane by two methods: 1) the hydrogen permeated through the Pd layer or 2) the hydrogen leaked through the flaws in the Pd layer. The values displayed in both plots are the percentages of hydrogen found on the permeate side of the membrane as a result of leakage. It is important to note that the values are based solely on the hydrogen content from the permeate gas

samples. Therefore, the percentage of hydrogen that permeated through the membrane is simply the plotted value subtracted from 100%. The feed and permeate results for nitrogen and hydrogen from each experiment were used in Eqn. (4-4) to find the data points shown in Figure 5-9 and Figure 5-10. The uncertainty analysis as stated in Chapter 4 was applied and can be seen in both figures.

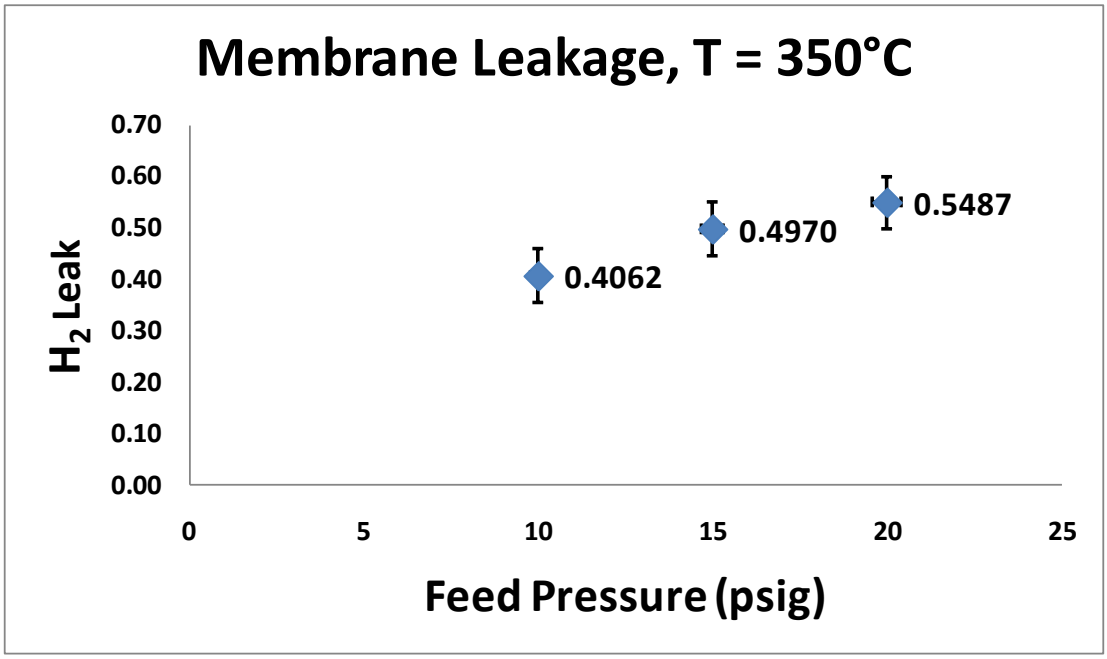

FIGURE 5-9. Hydrogen leak percentage vs. feed pressure at constant temperature.

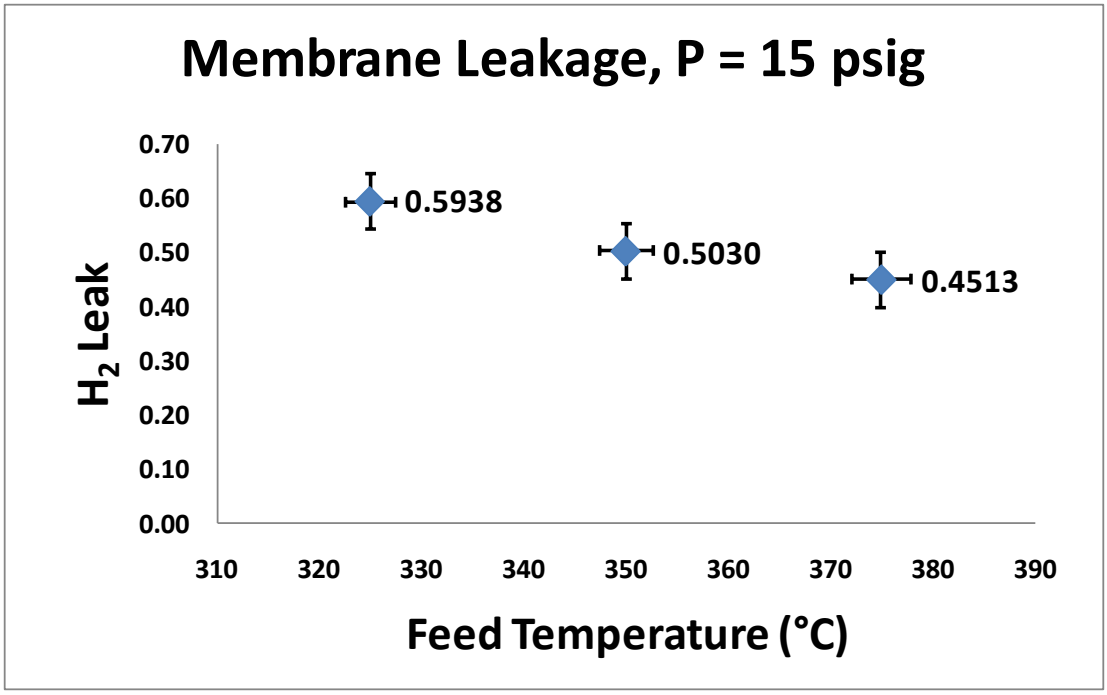

FIGURE 5-10. Hydrogen leak percentage vs. temperature at constant feed pressure.

The data displayed in Figure 5-9 shows that hydrogen leakage increases as the feed pressure rises (thus causing an increase in the hydrogen partial pressure difference). Conversely, the percentage of hydrogen permeated decreases with pressure increase. A different trend is shown in Figure 5-10, where hydrogen leakage decreases as temperature rises. This corresponds to a rise in the percentage of hydrogen permeated with temperature increase at a constant pressure. However, the trends found in Figures 5-9 and 5-10 needed to be reinforced through further examination.

Determination of the gas flux values was the next step in the analysis process. In order to find the individual flux values, each adjusted flow rate had to be found. The values recorded for the flowmeters in the experimental setup were the reference values. Each value had to be corrected based on the range of the flowmeter. This

was done using information provided by the manufacturer to make a curve fit plot. The converted reference values were found for air with units of cm^3/min (ccm) and will be referred to as the gauge values. The gauge values had to then be converted to the actual flow rates. This required knowing the molecular weight of the mixture. Finding the molecular weight of the mixture was accomplished by multiplying the mole fraction (given by the GC) by the molecular weight of each individual component and summing the values together. The actual volumetric flow rate of the mixture was then found using the below relation from the ideal gas law.

$$Q_a = Q_g \left(\frac{P_g}{P_a}\frac{T_a}{T_g}\frac{MW_g}{MW_a}\right)^{1/2} \tag{5-4}$$

The subscript "a" represents the actual values while "g" represents the gauge values. The gauge values for the pressure, temperature, and molecular weight terms are the values at which the gauge was calibrated. Once the actual flow for the mixture was found, the mole fraction values given by the GC were then used to find the individual component flow rates.

Using the actual hydrogen flow rate on the permeate side, the value was divided into permeated H_2 flow and leaked H_2 flow. This was based on the hydrogen flow percentages seen in Figures 5-9 and 5-10. With the copper washers in place, the diameter of the permeable area was reduced to 5/8 inch. The fluxes were calculated using the flow information and the permeable area of the membrane. The volumetric fluxes for N_2 $(Q_{N_2,L})$, H_2 leaked $(Q_{H_2,L})$ and H_2 permeated $(Q_{H_2,P})$ were calculated using the same area and are shown in Figures 5-11 and 5-12 below.

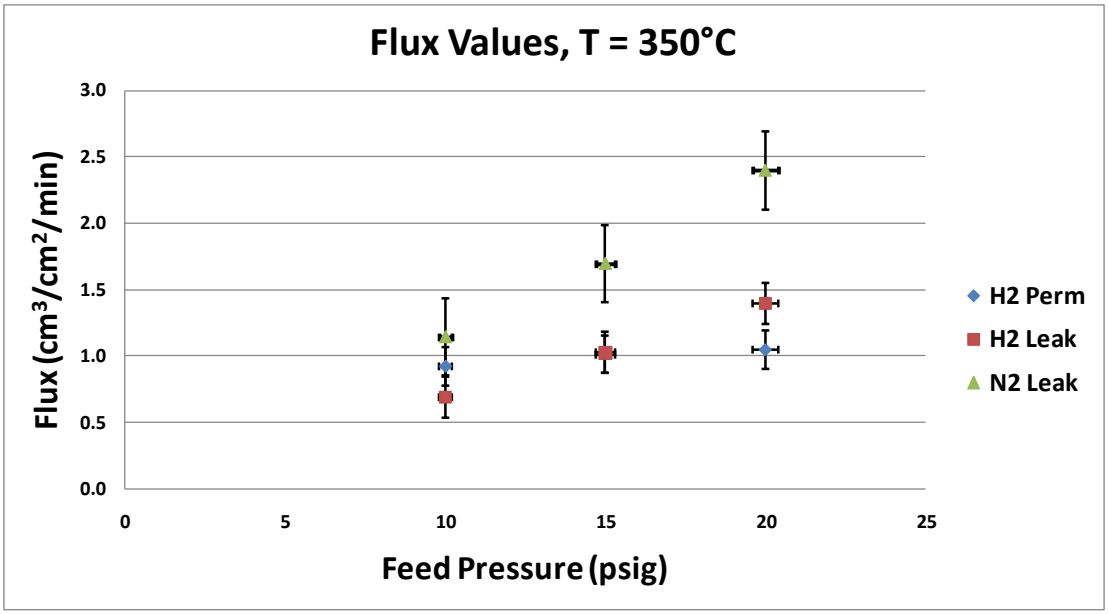

FIGURE 5-11. Volumetric flux values for constant temperature.

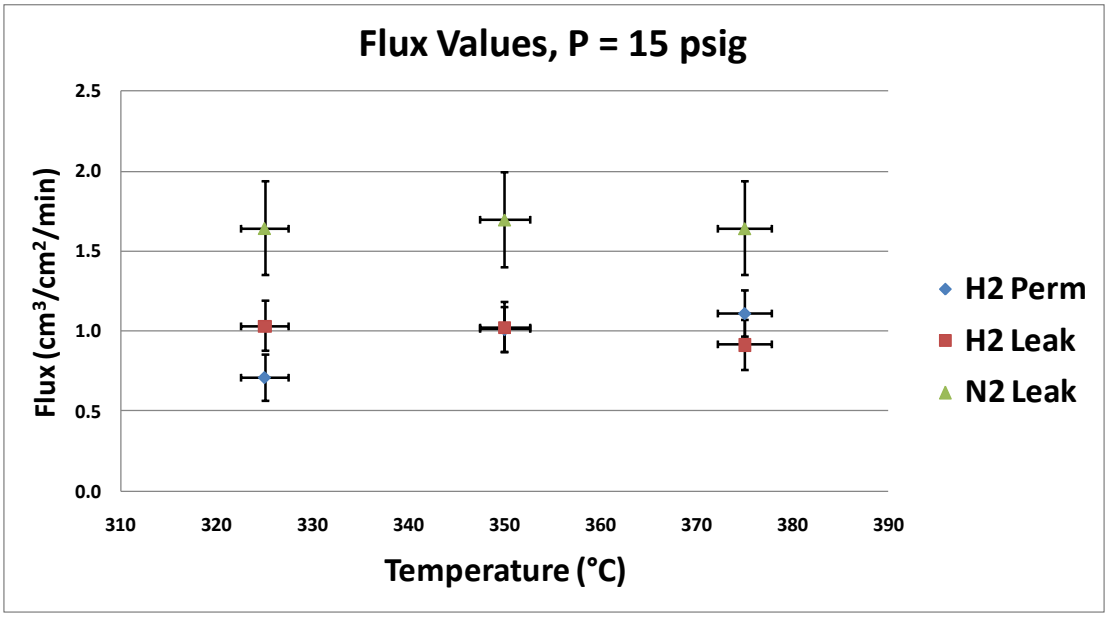

FIGURE 5-12. Volumetric flux values for constant pressure.

A direct correlation can be made between the data shown in Figures 5-11 and 5-12 and the trends in Figures 5-9 and 5-10. With temperature held constant, Figure 5-11 shows the hydrogen permeation flux increasing slightly with rising pressure

when compared to the rising hydrogen leak flux. Simultaneously, the nitrogen leak flux increases much more drastically than either hydrogen flux. On the other hand, Figure 5-12 shows that when pressure is constant the hydrogen permeation flux increases while the hydrogen leak flux decreases with rising temperature. The nitrogen leak flux experiences a relatively small change. This would not be the case if nitrogen was permeating through the membrane. For one, it has long been stated that palladium is permeable only to hydrogen. Secondly, nitrogen permeation would cause the nitrogen flux to follow a similar trend as the hydrogen permeation flux. Per Eqn. (2-8), the nitrogen flux should increase with rising temperature. However, since it remains relatively constant with increasing temperature, it can be concluded that the nitrogen on the permeate side is the result of faults in the Pd layer and not permeation.

The rise in hydrogen permeation flux with pressure comes as no surprise as the pressure is the driving force. The increasing hydrogen permeation flux with temperature is due to the temperature dependence of the diffusion constant and Sievert's constant in Eqn. (2-8). The behavior of the plots for the hydrogen permeate and leak fluxes in Figures 5-11 and 5-12 concur with the hydrogen leakage percentages displayed in Figures 5-9 and 5-10.

The next step in the analysis process was finding the hydrogen selectivity of the membrane. The selectivity is merely just the hydrogen permeation flux divided by the nitrogen leak flux [27]. The selectivity values for each experiment are plotted below in Figures 5-13 and 5-14. The trends shown are concurrent with the previous statements. Rising pressure causes the selectivity of the membrane to decrease while

increasing temperature improves the selectivity of the membrane. The decreasing selectivity can be attributed to the much greater increase in nitrogen flux compared to hydrogen permeation flux at constant temperature and rising pressure. The contrary is true for the rising selectivity, where the nitrogen leak flux remains relatively constant while the hydrogen permeation flux increases.

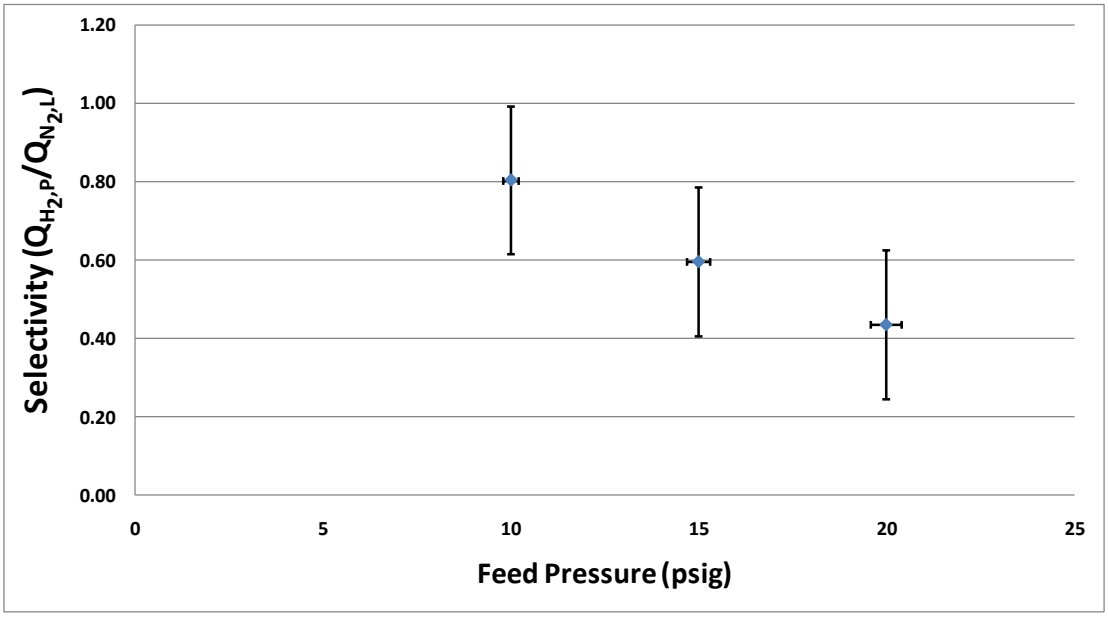

FIGURE 5-13. Selectivity values for T=350 degrees C.

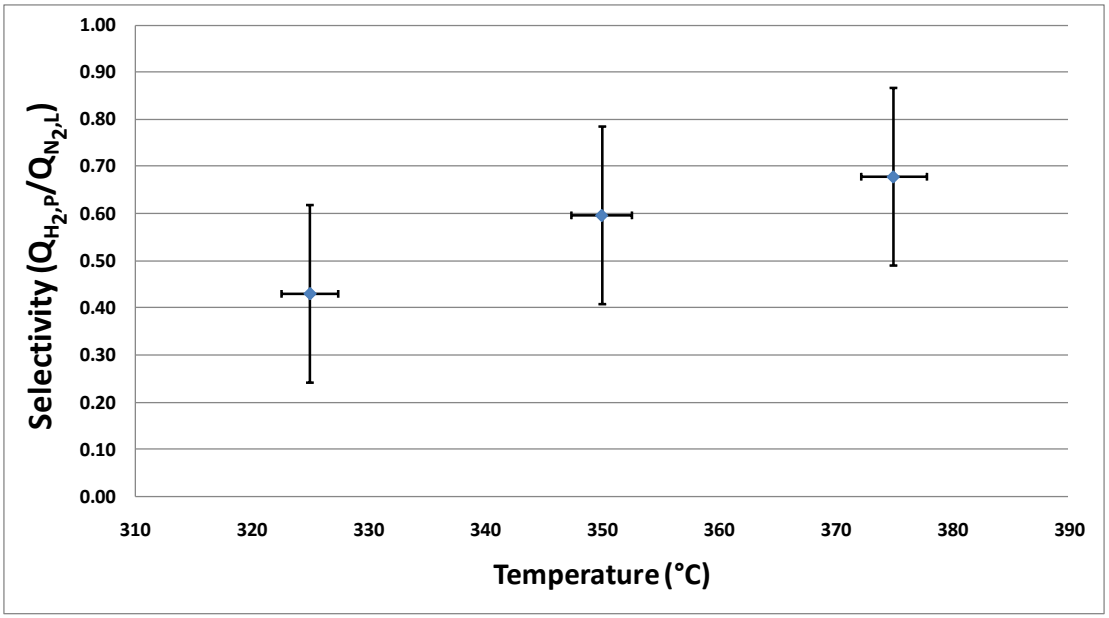

FIGURE 5-14. Selectivity values for P=15 psig.

5.3.3 Determining the Pressure Exponent and Activation Energy

The n-value on the right hand side of Eqn. (2-8) generally correlates to the rate limiting step of the diffusion process. In the case of n = 0.5, the rate limiting step is the bulk diffusion transport mechanism, while a pressure exponent of 1.0 indicates that the surface reaction is rate limiting [8]. When the pressure exponent is between 0.5 and 1.0, it is thought that a combination of both the surface reaction and hydrogen diffusion contribute to controlling the hydrogen permeation process [8]. In order to more accurately capture a trend for the pressure exponent, five additional experiments were conducted at T = 350 degrees C and feed pressures of 5, 10, 15, 20, and 25 psig. For this set of experiments, the molar hydrogen permeation flux was plotted versus the difference between the upstream and downstream hydrogen partial pressures raised to the power of n. Initially the plot range was 0.5 to 1.0 for n as shown in Figure 5-15, but the range was gradually reduced until the best fit was achieved. The

linear regression analysis revealed a pressure exponent of 0.82 with an R^2 value of 0.934. It is important to note, however, this value was determined at one temperature and that additional experiments at different temperatures may cause some minor variation in the n-value.

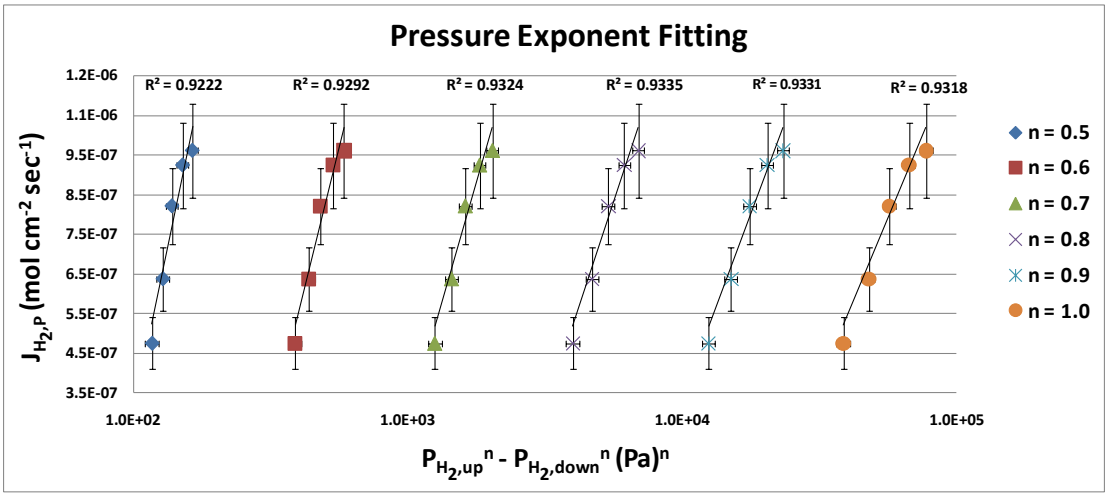

FIGURE 5-15. Molar hydrogen permeation flux vs. the difference in partial pressures to the n^{th} power. The values were plotted with varying n-values until the best linear fit was achieved.

Pressure exponents greater than 0.5 in Pd membranes with known defects are to be expected due to the hydrogen leakage through compromised areas of the membrane [27]. With a pressure exponent of 0.82, the rate limiting step of Membrane IV is a combination of the diffusion process and surface interferences. The use of a support for the Pd layer could be a likely cause of surface site obstruction. The support can block sites on the downstream side of the Pd layer where hydrogen atoms would otherwise recombine [21]. The use of an argon sweep gas could potentially cause some impedance if argon ventures into any of the pores on the support [21]. The presence of leaking nitrogen inside the porous stainless steel

support could also inhibit the diffusion of hydrogen in the same way as the argon sweep gas.

Finding the n-value corresponding to the pressure term in Eqn. (2-8) provided a better understanding of the pressure dependency of the permeation process in addition to the rate limiting step. Finding the temperature dependency, which is absorbed into the D and K terms of Eqn. (2-8), led to the determination of the activation energy and the permeability constant. These two terms can be combined to form what is known as the permeability term, k [8,27].

$$k = k_0 exp\left(-\frac{E}{RT}\right) \tag{5-5}$$

The k_0 term in Eqn. (5-5) is the permeability constant, the R is the gas constant, and the E is the activation energy of the palladium membrane. Rewriting Eqn. (2-8) with the Arrhenius relation as shown in Eqn. (5-5) yielded a new relation for Fick's law as shown below.

$$J_{H_2} = \frac{k_0}{2X_M} \exp\left(-\frac{E}{RT}\right)\left(P_{H_2}^n, up - P_{H_2}^n, down\right) \tag{5-6}$$

The k_0 and x_m terms in Eqn. (5-6) are constants and all other terms are known or can be solved. The right hand side of the equation is multiplied by one half in order to account for the flux of hydrogen molecules instead of hydrogen atoms. Rearranging Eqn. (5-6) as shown below allows for the molar flux to be plotted versus inverse temperature in order to find the activation energy.

$$\ln\left(\frac{J_{H_2}}{\Delta \mathrm{P}}\right) = \ln(C) - \frac{E}{RT} \tag{5-6}$$

$$C = \frac{k_0}{2X_M}, \Delta \mathrm{P} = P_{H_2}^n, up - P_{H_2}^n, down$$

The relation in Eqn. (5-6) is displayed in Figure 5-16 below. Linear regression was used to find an equation relating the natural log of the flux and pressure change (y) to the inverse temperature (x).

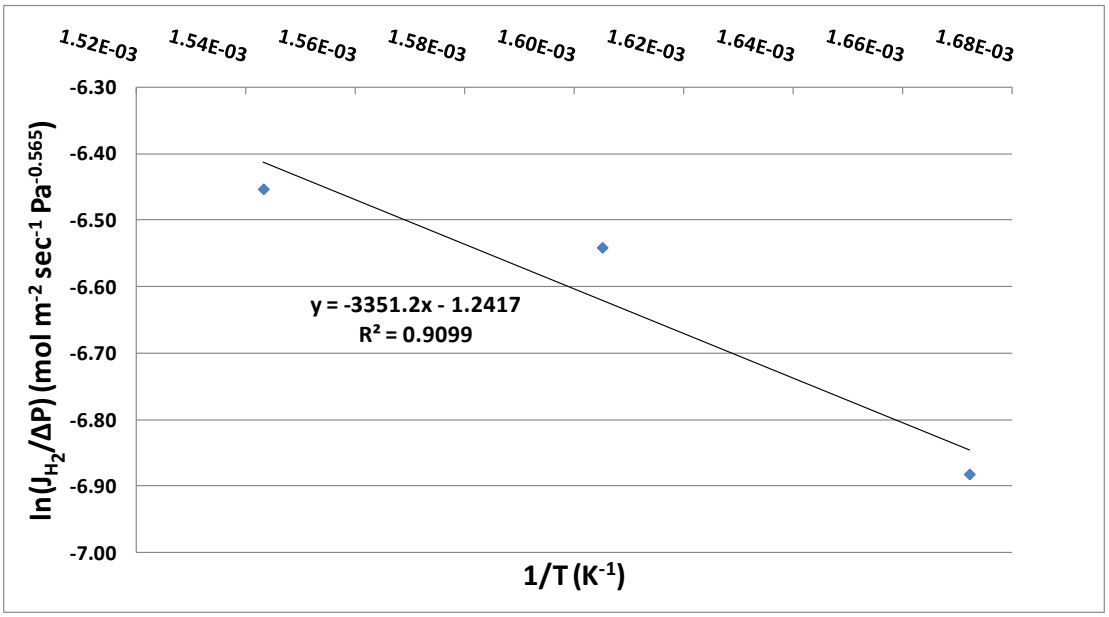

FIGURE 5-16. Method to determine the activation energy of the Pd membrane.

Using $y = ax + b$ for the equation of the line in Figure 5-16, the coefficients "a" and "b" can be defined as follows: $a = \frac{E}{R}$ and $b = C$ as defined above. Therefore, the activation energy and permeability constant values for Pd Membrane IV are as follows:

$$E = 28.13 \ {}^{kJ}/_{mol}$$

$$k_0 = 3.532E-9 \ {}^{mol}/_{m \cdot s \cdot Pa^{0.82}}$$

The value for the activation energy is on the same order of magnitude as many of the values found in the literature for pure Pd membranes. Examples of what other researchers have found are displayed in Table 5-1. As can be seen in the table, the

values found by other researchers for membranes of similar thickness tend to be similar in value to what was found for Membrane IV.

Membrane Thickness (X_m)	Activation Energy (E)	Source
13 µm	10.7 kJ/mol	Uemiya [17]
6 µm	19 kJ/mol	Huang [21]
15 µm	13 kJ/mol	Huang [21]
20 µm	10 kJ/mol	Huang [21]
10 µm	7.1 kJ/mol	Wang [22]

Table 5-1. Activation Energy values found in the literature for Pd membranes.

Knowing the activation energy for Membrane IV makes it known the energy required for hydrogen separation to take place. As shown in Table 5-1, some studies suggest that the activation energy decreases with increasing membrane thickness [21]. However, lower activation energies have been found for some thin membranes and are also shown in Table 5-1 [17,22].

5.4 Discussion of Results

The hydrogen permeation data found as a result of the experiments conducted in this study is similar to what is generally found in the literature. The hydrogen permeation flux increased with both rising temperature and increasing partial pressure difference, demonstrating its dependence on both temperature and pressure. However, the permeation flux values were directly impacted by the presence of leaks in the Pd layer of the membrane. These leaks had the most adverse effects on the hydrogen permeation flux as the partial pressure difference increased. Conversely, increasing the system temperature had the least impact on the hydrogen permeation flux.

The nitrogen flux did not change much with pressure held constant and rising temperature, but conversely had the most drastic increase when pressure was elevated with constant temperature. The trends shown in Figures 5-9 and 5-10 indicate that hydrogen permeation benefits mostly with a temperature increase rather than a pressure increase when leaks are present. This is confirmed by the flux plots in Figures 5-11 and 5-12 and the selectivity values in Figures 5-13 and 5-14.

The increasing hydrogen leakage with rising pressure shows that the hydrogen is diffusing through the porous media much faster than it is permeating through the Pd layer. This is confirmed in Figure 5-11, where all three flux values are shown to be increasing with pressure. However, the hydrogen leak flux and the nitrogen flux increase at a significantly higher rate than the hydrogen permeation flux. It is expected that gas transfer through porous media will occur faster than permeation as the partial pressure difference increases.

Comparing the effect of increasing temperature to the flux values draws a different conclusion than the one stated in the previous paragraph. The hydrogen permeation flux increases with rising temperature, but the hydrogen leak flux decreases while the nitrogen leak flux remains relatively constant, as shown in Figure 5-12. This means that the effect of temperature is greater on the hydrogen permeation than it is on both hydrogen and nitrogen transport through the porous media wherever there are faults in the Pd layer. The decrease in the hydrogen leak flux suggests that the temperature increase promotes greater hydrogen adsorption on the surface of the Pd layer. This increased adsorption causes a greater amount of hydrogen molecules

to traverse through the membrane via the permeation process rather than by transport through the porous support.

The reaction was found to be both surface limiting and diffusion limiting as suggested by the pressure exponent value of 0.82. Surface limiting effects, such as the decreased availability of active sites on the downstream side of the Pd layer due to the porous support, were discussed in the previous section. However, there is also the possibility that the surface reaction could be limited on the upstream side of the membrane as well. Section 2.5 discussed at length the effect of feed stream impurities on hydrogen permeation. Specifically, Section 2.5.1 focused on the negative impact of the presence of nitrogen in the feed stream. It is rather likely that nitrogen molecules were attaching themselves to the active sites on the upstream side of the Pd membrane during the experiments in this study. However, experiments were not conducted for long enough periods of time to study the effects of nitrogen at the surface of the membrane. The primary reason for the diffusion limiting aspect of the reaction is due to the presence of other gases in the porous support. The effect of having argon entering pores from the sweep side as well as nitrogen transport through defects on the feed side creates several interferences for hydrogen atoms traversing through the membrane.

As a closing note, some additional experiments were conducted using a Pd/Cu membrane. The results are shown in Appendix C and are compared to the results from Membrane IV testing. This additional study was conducted purely to provide a reference point for future work and is not specifically tied to any of the conclusions made in this thesis.

Chapter 6: Recommendations for Future Work

Several observations for improvement were made during both the design and experimental portions of this project. This chapter will focus on detailing these observations and the associated recommendations. The recommendations will be divided into two sections. One section will focus on modifications to the facility, including the membrane housing. The second section will be dedicated to suggestions for future experimental analysis.

6.1 Hydrogen Separation Facility Improvements

Achieving a good pressure seal when assembling the membrane housing was possible when a third washer was used instead of a membrane. Once a membrane was placed in the casing gas was able to leak through the porous support in the radial direction. Since use of the Novatec gasket proved to be ineffective, there is another technique that should be considered during future use of the membrane housing. Instead of placing the membrane between the two copper washers, a pressure seal is more likely if the membrane is placed directly in the feed side of the casing and held in place with the two copper washers behind it. This way the Pd side of the membrane is seated in the feed side and the edges of the porous support are pressed against the inner wall of the casing. This would have no effect on the casing assembly and it can be conducted in same manner as was described in Chapter 3. The only exception would be that the membrane and feed side copper washer would switch places. In order for this to be possible, however, the washer seating lip on the

feed side component of the housing would most likely need to be machined a few thousandths of an inch larger in diameter. It is also important to note that the Pd side of the membrane stuck to the copper washer after experiments at elevated temperatures. When the two were separated, some of the Pd came off on the copper washer. If this occurs when the Pd is put in contact with the stainless steel, the membrane could become stuck in the feed side component.

6.2 Future Experimental Work

The determination of the pressure exponent in Chapter 5 was done at one temperature over a range of varying partial pressure differences. To further solidify, or determine, the n-value for Membrane IV it is recommended that additional experiments be conducted at several other constant temperature values. This will give a few more data points on which to base a trend in determining the n-value. It is unlikely that the n-value will be drastically different, but it may change slightly enough as to yield a lower R^2 value.

One of the underlying assumptions in these experiments was that the hydrogen to nitrogen ratio in the feed gas was constant as it leaked through the defects in the membrane. This theory should be tested by running several gas mixtures through the facility without the presence of hydrogen. This will not only test the theory that the ratio remains constant, but it will also check to see if there is any difference in behavior through the leaks between any of the gas mixtures. In other words, test to see if one gas tends to be more or less dominant than any other gas when diffusing through the porous support.

A third recommendation is that the surface effects of co-existing gases in the feed mixture be examined. This is important in determining the performance of the membrane over an extended period of time when subjected to gases other than hydrogen. If a degradation in hydrogen flux is detected in the presence of other gases, then it should be determined if this is a lasting or temporary effect. If it is a lasting effect, then a method by which to restore the membrane to its initial permeation capability should also be explored. Along the same lines, the impact of running a hydrogen lean mixture over the membrane for a period of time could result in lower hydrogen permeation values for a hydrogen rich mixture applied immediately afterwards. This is relative to the membrane surface activity and should be studied if this problem arises.

The final recommendation involves the membrane composition. Any of the previously stated recommendations can be applied for any membrane. Using membranes that differ in material composition for testing can greatly enhance the amount of knowledge gained regarding membrane performance. In a world where the search for cheaper, more efficient and more reliable energy sources is of increasing importance, the value of a better understanding of membrane usage for hydrogen separation is limitless. The results from some preliminary testing on a Pd/Cu membrane can be seen in Appendix C. Expanding the studies beyond the scope of the experiments conducted here and comparing to what others are doing can lead to valuable information moving forward.

Appendix A: Membrane Casing Design Drawings

The line drawings depicting the dimensions and details of the membrane housing are included in this appendix.

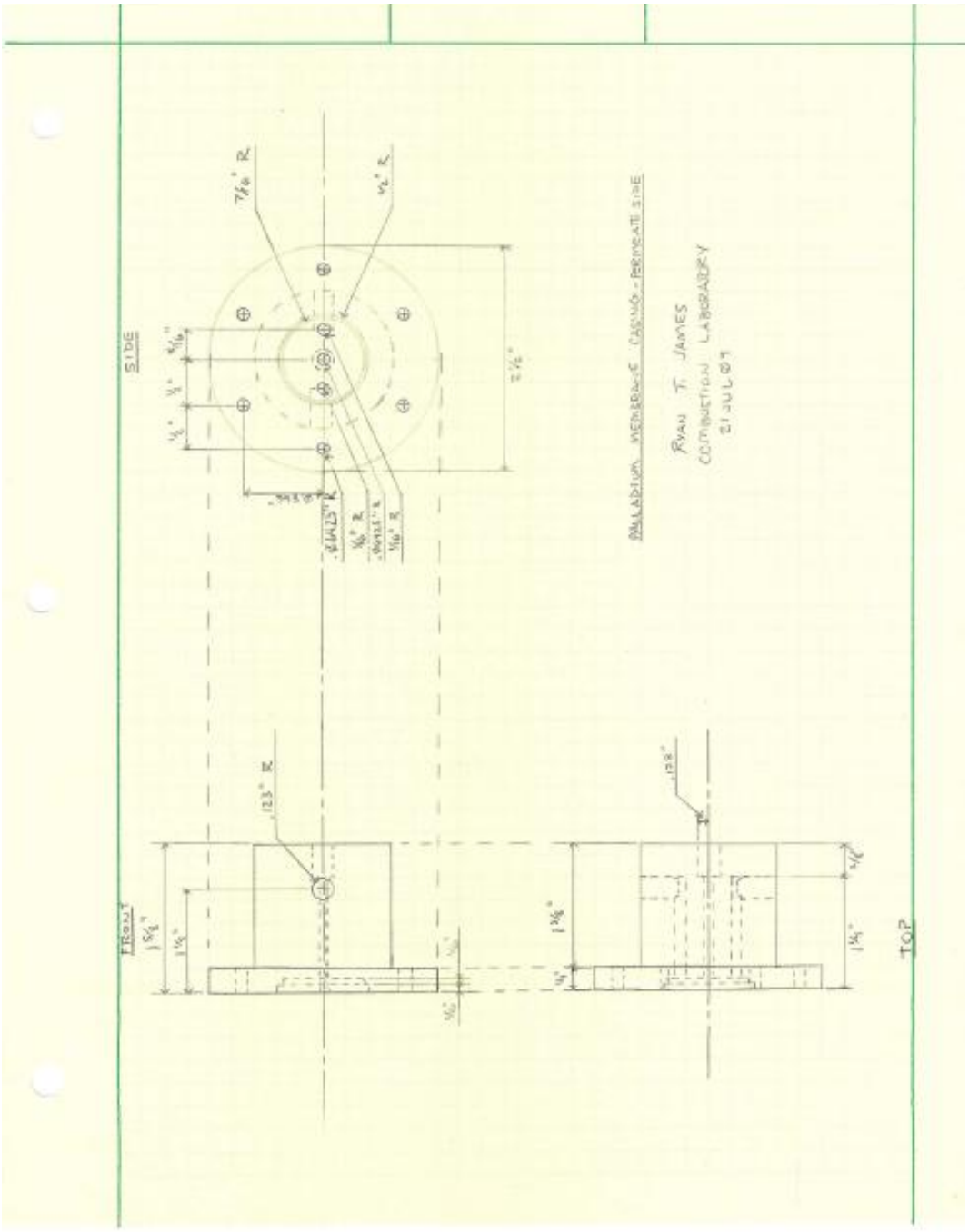

Figure A-1. Three view engineering drawing of the sweep component of the membrane casing.

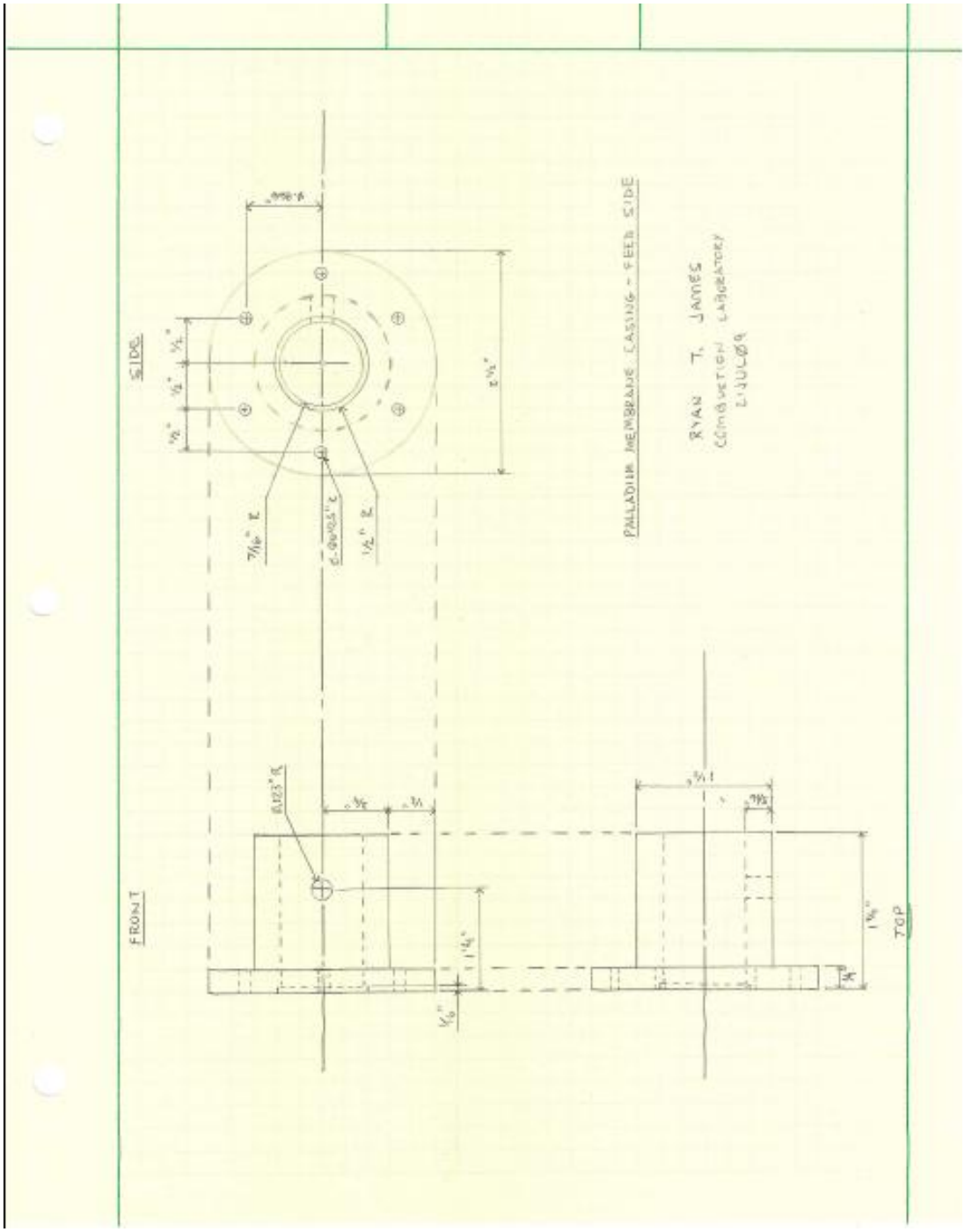

Figure A-2. Three view engineering drawing of the feed component of the membrane casing.

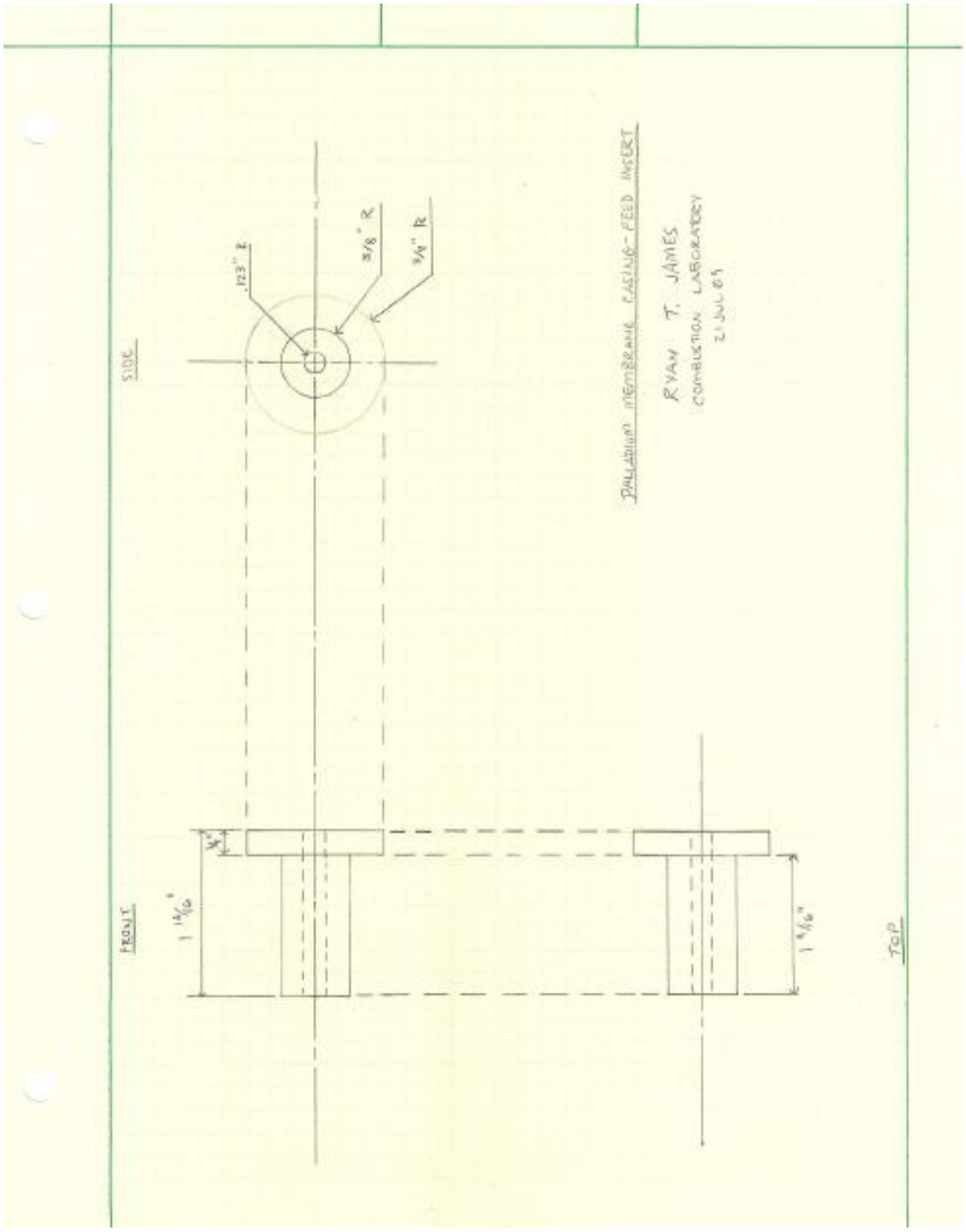

Figure A-3. Three view engineering drawing of the feed insert component of the membrane casing.

Appendix B: Housing Assembly

As was explained in Section 3.2, the order in which the screws are tightened is important to ensure that they are tightened uniformly. Figure B-1 below displays the order in which the screws should be tightened using a torque screwdriver. Each screw should have the same amount of torque applied to it, but not so much that one side is tight and the other side is loose. The number of time around it takes to tighten the casing can vary, but generally should take 4 to 6 rounds.

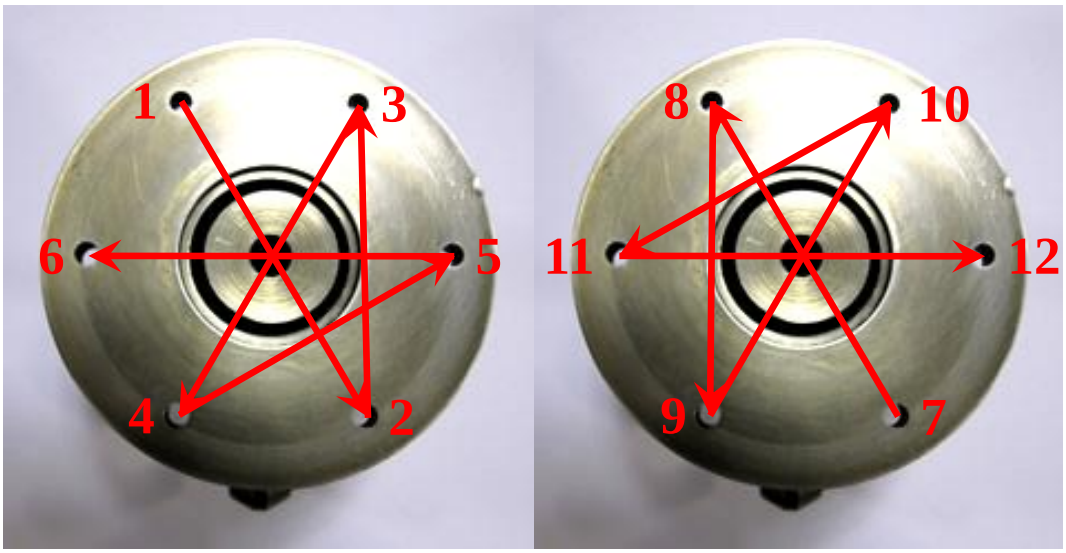

(a) **(b)**

FIGURE B-1. Machine screw tightening order on the first round (a) and second round (b). The order is such that each screw is tightened opposite each other while moving in a clockwise direction.

Appendix C: Pd/Cu Membrane Testing

After completion of the work provided in support of this thesis, some additional experiments were conducted using a Pd/Cu membrane provided by Dr. Ilias's research team at NC A&T. As was stated at the end of Chapter 5, these results have no direct correlation to any of the conclusions drawn in this thesis and are provided solely as a reference point for future work.

The experiments on the Pd/Cu membrane were carried out in the same manner as the previous studies conducted on Membrane IV. Prior to testing, the membrane was examined under a microscope at 30x magnification. The surface layer appeared to be in better condition than Membranes I through IV. However, upon initial testing it was discovered that nitrogen leaked through the membrane to the permeate side. The experiments for the Pd/Cu membrane (Membrane VII) were conducted at a temperature of 350 degrees C and feed pressures of 5, 10, 15, 20 and 25 psig. The molar flux values were then calculated in the same manner as with the results for Membrane IV. The comparison between the molar flux values for Membrane IV and Membrane VII can be seen in Figure C-1 below.

Based on the results found in the literature, it is generally expected that the Pd/Cu membrane should perform better than the pure Pd membrane. However, this is for the best case when the Pd/Cu alloy comprises of 40% Cu in the Pd. As can be seen in Figure C-1, the Pd membrane outperforms the Pd/Cu membrane at each feed pressure increment with the exception of the last one (25 psig). The amount of copper in this alloy membrane is unknown and therefore the Pd/Cu membrane may

actually underperform when compared to the pure Pd membrane. Another explanation is that Pd based membranes sometimes require a significant amount of time to fully activate and reach peak permeation rates. The results for the pure Pd membrane shown below are after 40+ hours of operation whereas the results for the Pd/Cu membrane are after only 4+ hours of operation.

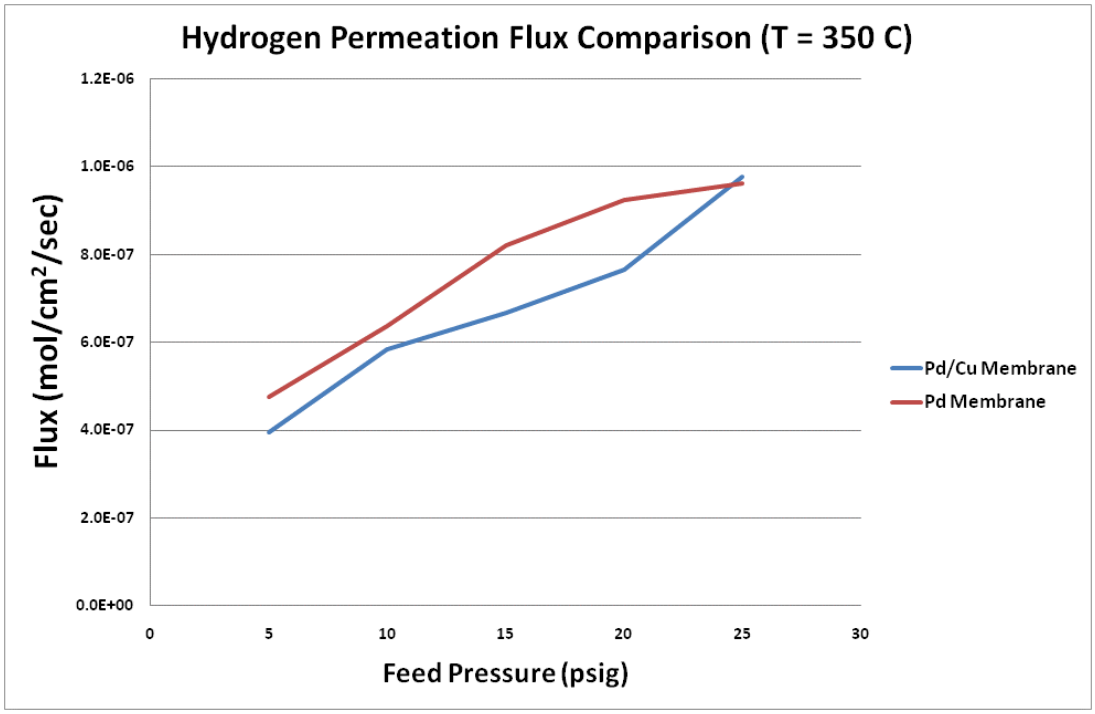

FIGURE C-1. Comparison of hydrogen permeation molar flux values for both the Pd/Cu membrane (red) and the pure Pd membrane (blue).

Further testing is required once Membrane VII has been run through additional hydrogen separation cycles. Once the operational times are similar, more reasonable comparisons can be made between the molar flux values. This coincides with the recommendations made in Chapter 6. Additional experiments with temperature variation to determine the pressure exponent and activation energy would also be helpful when comparing the pure Pd and Pd/Cu membranes.

Bibliography

[1] G.J. Grashoff, C.E. Pilkington, and C.W. Corti. "The purification of hydrogen: A review of the technology emphasizing the current status of palladium membrane diffusion." *Platinum Metals Review* 27 (4) (1983): 157-169.

[2] J.B. Hunter. "Silver-palladium film for separation and purification of hydrogen." U.S. Patent 2,773,561. 11 Dec. 1956.

[3] A. Unemoto, K. Atsushi, K. Sato, T. Otake, K. Yashiro, J. Mizusaki, T. Kawada, T. Tsuneki, Y. Shirasaki, and I. Yasuda. "Surface reaction of hydrogen on a palladium alloy membrane under co-exisence of H_2O, CO, CO_2, or CH_4." *International Journal of Hydrogen Energy* 32 (2007): 4023-4029.

[4] A.C. Makrides, M.A. Newton, H. Wright and D.N. Jewett. "Separation of hydrogen by permeation." U.S. Patent 3,350,846. 7 Nov. 1967.

[5] S. Wilke and M. Scheffler. "Potential-energy surface for H_2 dissociation over Pd(100)." *Physical Review* 53.8 (1996): 4926-4932.

[6] L. Zaluski, A. Zaluska, P. Tessier, J.O. Strom-Olsen, and R. Schulz. "Catalytic effect of Pd on hydrogen absorption in mechanically alloyed Mg_2Ni, $LaNi_5$ and FeTi." *Journal of Alloys and Compounds* 217 (1995): 295-300.

[7] T. Mitsui, M.K. Rose, E. Fomin, D.F. Ogletree, and M. Salmeron. "Dissociative hydrogen adsorption on palladium requires aggregates of three or more vacancies." *Letters to Nature* 422 (2003): 705-707.

[8] B.D. Morreale, M.V. Ciocco, R.M. Enick, B.I. Morsi, B.H. Howard, A.V. Cugini, and K.S. Rothenberger. "The permeability of hydrogen in bulk palladium at elevated temperatures and pressures." *Journal of Membrane Science* 212 (2003): 87-97.

[9] D.L.McKinley and W. Nitro, U.S. Patent 3,247,648. 26 April 1966.

[10] N.M. Peachey, R.C. Snow, and R.C. Dye. "Composite Pd/Ta metal membranes for hydrogen separation." *Journal of Membrane Sciences* 111 (1996): 123-133.

[11] R.E. Buxbaum and T.L. Marker. "Hydrogen Transport through non-porous membranes of palladium-coated niobium, tantalum, and vanadium." *Journal of Membrane Sciences* 85. (1993): 29-38.

[12] A.G. Knapton. "Palladium alloys for hydrogen diffusion membranes." *Platinum Metals Review* 21 (2) (1977): 44-50.

[13] J.E. Philpott. "Hydrogen diffusion technology: commercial applications of palladium membranes." *Platinum Metals Review* 29 (1) (1985): 12-16.

[14] M.L. Doyle and I.R. Harris. “Palladium-rare earth alloys.” *Platinum Metals Review* 32 (1988): 130-140.

[15] S. Ilias, N. Su, U.I. Udo-Aka and F.G. King. “Application of eletroless deposited thin-film palladium composite membrane in hydrogen separation.” *Separation Science and Technology* 32 (1997): 487-504.

[16] B.H. Howard, R.P Killmeyer, K.S. Rothenberger, A.V. Cugini, B.D. Morreale, R.M. Enick and F. Bustamante. “Hydrogen permeance of palladium-copper alloy membranes over a wide range of temperatures and pressures.” *Journal of Membrane Science* 241 (2004): 207-218.

[17] S. Uemiya, Y. Kude, K. Sugino, N. Sato, T. Matsuda and E. Kikuchi. “A palladium/porous-glass composite membrane for hydrogen separation.” *Chemistry Letters* (1988): 1687-1690.

[18] F. Gielens, R. Knibbeler, P. Duysinx, H. Tong, M. Vortsman and J. Keurentjes. “Influence of steam and carbon dioxide on the hydrogen flux through thin Pd/Ag and Pd membranes.” *Journal of Membrane Science* 279 (2006): 176-185.

[19] H. Tong, J. Berenschot, M. De Boer, J. Gardeniers, H. Wensink, H. Jansen, W. Nijdam, M. Elwenspoek., F. Gielens and C. van Rijn. “Microfabrication of palladium-silver alloy membranes for hydrogen separation.” *Journal of Microelectromechanical Systems* 12.5 (2003): 622-629.

[20] J. Okazaki, T. Ikeda, D.A. Tanaka, M.A. Tanco, Y. Wakui, K. Sato, and F. Mizumkami. “Importance of the support material in thin palladium composite membranes for steady hydrogen permeation at elevated temperatures.” *Physical Chemistry Chemical Physics* 11 (2009): 8632-8639.

[21] Y. Huang and R. Dittmeyer. “Preparation of thin palladium membranes on a porous support with rough surface.” *Journal of Membrane Science* 302 (2007): 160-170.

[22] D. Wang, J. Tong, H. Xu and Y. Matsumura. “Preparation of palladium membrane over porous stainless steel tube modified with zirconium oxide.” *Catalysis Today* 93-95 (2004) 698-693.

[23] C. van Rijn, M. Wekken, W. Nijdam and M. Elwenspoek. “Deflection and maximum load of microfiltration membrane sieves made with silicon micromachining.” *Journal of Microelectromechanical Systems* 6.1 (1997): 48-54.

[24] W. Wang, X. Pan, X. Zhang, W. Yang and G. Xiong. “The effect of co-existing nitrogen on hydrogen permeation through thin Pd composite membranes.” *Separation and Purification Technology* 54 (2007): 262-271.

[25] F. Sakamoto, Y. Kinari, F. Chen and Y. Sakamoto. “Hydrogen permeation through palladium alloy membranes in mixture gases of 10% nitrogen and

ammonia in the hydrogen." *International Journal of Hydrogen Energy* 22.4 (1997): 369-375.

[26] F. Gallucci, F. Chiaravalloti, S. Tosti, E. Drioli and A. Basile. "The effect of mixture gas on hydrogen permeation through a palladium membrane: experimental study and theoretical approach." *International Journal of Hydrogen Energy* 32 (2007): 1837-1845.

[27] F. Guazzone, E. Engwall and Y. Ma. "Effects of surface activity, defects and mass transfer on hydrogen permeance and n-value in composite palladium-porous stainless steel membranes." *Catalysis Today* 118 (2006): 24-31.

[28] "Novatec PREMIUM II." Frenzelit Sealing Systems. Last accessed March 24, 2010, from http://www.frenzelitsealing.com/968_novatec_premium_ii.html.

[29] "General Service Pressure Gauge." McMaster-Carr. Last accessed March 24, 2010, from http://www.mcmaster.com/#atmospheric-pressure-gauges/=6dh029.

[30] Omega Engineering, Inc. Last accessed March 24, 2010, from http://www.omega.com/.

[31] "Palladium Foil." Goodfellow Corporation. Last accessed March 24, 2010, from https://www.goodfellowusa.com/catalog/.